

Supporting Information  
for DOI: 10.1055/a-1941-7757  
© 2022. The Author(s).  
Georg Thieme Verlag KG, Rüdigerstraße 14, 70469 Stuttgart, Germany

# An Azobenzene-Clamped Bichromophore

Nils Schmickler<sup>a</sup>, David A. Hofmeister<sup>a</sup>, Joshua Bahr<sup>a</sup>, Jakob Schedlbauer<sup>b</sup>, Stefan-S. Jester<sup>a\*</sup>,  
John M. Lupton<sup>b\*</sup>, Sigurd Höger<sup>a\*</sup>

<sup>a</sup> Kekulé-Institut für Organische Chemie und Biochemie  
Rheinische Friedrich-Wilhelms-Universität Bonn  
Gerhard-Domagk-Str. 1, 53121 Bonn; Germany  
E-Mail: hoeger@uni-bonn.de; stefan.jester@uni-bonn.de

<sup>b</sup> Institut für Experimentelle und Angewandte Physik  
Universität Regensburg  
Universitätsstrasse 31, 93053 Regensburg Germany  
E-mail: john.lupton@physik.uni-regensburg.de

## Supporting Information

1	General	S3
1.1	Reagents and analytics	S3
1.2	Gel permeation chromatography	S3
1.3	Scanning tunneling microscopy	S4
1.4	(Supra-) molecular modelling	S4
1.5	Optical spectroscopy	S4
2	Synthesis of halogenated hydroquinone dialkylethers	S6
3	Synthesis of <b>4</b>	S9
4	Synthesis of <b>1</b>	S13
5	Additional molecular models and scanning tunneling microscopy images of <b>1</b> and <b>8</b>	S22
6	UV/vis spectra of <b>1</b> , <b>6b</b> , and <b>8</b>	S27
7	Thin layer chromatography of <b>6b</b> and <b>8</b>	S31
8	Methods for optical spectroscopy	S37
9	References	S38

## 1 General

### 1.1 Reagents and analytics

Reagents were purchased at reagent grade from commercial sources and used without further purification. All air-sensitive reactions were carried out using standard Schlenk techniques under argon. 2-Bromo-5-iodo hydroquinone (**8**) was prepared as described in Ref. [S1]. [(3-Cyanopropyl) diisopropylsilyl] acetylene (CPDiPS-acetylene) and [(3-cyanopropyl dimethylsilyl] acetylene (CPDMS-acetylene) were prepared as described in Ref. [S2]. Diiodo azobenzene (**2**) was prepared as described in Ref. [S3]. Reaction solvents (THF, piperidine, dichloromethane, pyridine, triethylamine, toluene) were dried, distilled, and stored under argon according to standard methods; workup solvents were either used in "p.a." quality or purified by distillation (dichloromethane, cyclohexane). Prior to characterization and further processing, all solids and oils were dried at rt under vacuum.  $^1\text{H}$  and  $^{13}\text{C}$  NMR spectra were recorded on a Bruker Avance I 300 MHz, Bruker Avance I 400 MHz, Bruker Avance III HD 500 MHz Prodigy and Bruker Avance III HD 700 MHz Cryo (300.1, 400.1, 500.1 and 700.1 MHz for  $^1\text{H}$  and 75.5, 100.6, 125.8 and 176.0 MHz for  $^{13}\text{C}$ ). Chemical shifts are given in parts per million (ppm) referenced to residual  $^1\text{H}$  or  $^{13}\text{C}$  signals in deuterated solvents. All NMR spectra were recorded at rt unless otherwise described. Mass spectra were measured on a Finnigan ThermoQuest MAT 95 XL (EI-MS), a Sektorfeldgerät MAT 90 (EI-MS), a Bruker Daltonics micrOTOF-Q (ESI-MS, APCI), a Bruker Daltonics autoflex TOF/TOF (MALDI-MS; matrix material: DCTB, no salts added) and an ultrafleXtreme TOF/TOF of the Bruker Daltonik company (MALDI-MS; matrix material: DCTB, no salts added). Thin layer chromatography was conducted on silica gel coated aluminium plates (Macherey-Nagel, Alugram SIL G/UV254, 0.25 mm coating with fluorescence indicator). Silica gel Kieselgel 60 (Merck, 0.040-0.063 mm) was used as the stationary phase for column chromatography.

### 1.2 Gel permeation chromatography

Gel permeation chromatography (GPC) was performed in THF (HPLC grade, stabilized with 2.5 ppm BHT) at rt. GPC analyses were run on an Agilent Technologies system at a flow rate of 1 mL/min using an IsoPump (G1310 A), a diode array UV detector (G1315B) and PSS columns (Polymer Standards Service, Mainz, Germany;  $10^2$ ,  $10^3$ ,  $10^5$  and  $10^6$  Å, 5  $\mu$ , 8  $\times$  300 mm). All molecular weights were determined vs PS calibration (PS standards from PSS, Mainz, Germany).

For the preparative separation, a Shimadzu Recycling GPC (rec GPC) system, equipped with an LC-20 AD pump, an SPD-20 A UV detector and a set of three preparative columns from PSS (either SDV  $10^3$  Å, 5  $\mu$ , 20  $\times$  300 mm or SDV preparative linear S, 5  $\mu$ , 20  $\times$  300 mm) with precolumn (SDV, 5  $\mu$ , 20  $\times$  50 mm) was employed. The system operated at a flow rate of 5 mL/min, THF, 35° C.

### 1.3 Scanning tunneling microscopy

Scanning tunneling microscopy (STM) was performed under ambient conditions (rt) at the solution/solid interface, using 1,2,4-trichlorobenzene (TCB) as solvent and highly oriented pyrolytic graphite (HOPG) as substrate. In a typical experiment, 0.2  $\mu\text{L}$  of a  $5 \times 10^{-6}$  M to  $1 \times 10^{-5}$  M solution of the compound of interest was dropped onto a freshly cleaved HOPG substrate at elevated temperature (80  $^{\circ}\text{C}$ ), kept at this temperature for 20 s, and allowed to cool to rt before the STM measurements were performed with the tip immersed into the solution. Bias voltages between -0.8 V and -1.2 V and tunneling current set points in the range of 26 pA to 117 pA were applied to image the supramolecular adlayers shown here. The experimental setup consists of an Agilent 5500 scanning probe microscope that is placed on a Halcyonics actively isolated microscopy workstation. It is acoustically shielded with a home-built box. Scissors cut Pt/Ir (80/20) tips were used and further modified after approach by applying short voltage pulses until the desired resolution was achieved. HOPG was obtained from TipsNano (*via* Anfatec) in ZYB-SS and DS quality. All STM images (unless otherwise noted) were calibrated by subsequent immediate acquisition of an additional image at reduced bias voltage, therefore the atomic lattice of the HOPG surface is observed which is used as a calibration grid. Data processing, also for image calibration, was performed using the SPIP 5 (Image Metrology) software package.

### 1.4 (Supra-) molecular modelling

(Supra-) molecular modelling was performed using Wavefunction Spartan '18. Equilibrium geometries shown in Figure S4 were obtained using molecular mechanics (based on the Merck Molecular Force Field (MMFF)) and a graphene monolayer with fixed atom positions as interaction partner. Equilibrium geometries shown in Figure S7b-g were obtained with the same method, however using three different starting geometries. These were manually created to match the shapes observed in the STM image shown in Figure S7a (arrows 1-6). Moreover, dihedral angles of the azobenzene units were frozen to obtain the *trans* or *cis* isomers. The molecular models shown in Figure 1c (Main Text) were obtained from the backbone structure shown in Figure S4a and b and subsequently added all-*trans* configured alkoxy side chains oriented along the HOPG main axis directions observed in the STM image, and these molecules were used to create the supramolecular model. The supramolecular model shown in Figure 1d (Main Text) was obtained in an alike procedure to match the structures observed in the STM image shown in Figure 1b (Main Text).

### 1.5 Optical spectroscopy

UV/vis absorption spectra shown in Figures S9 – S11 were recorded on a Perkin Elmer Lambda 18 spectrometer using 10 mm quartz cuvettes.

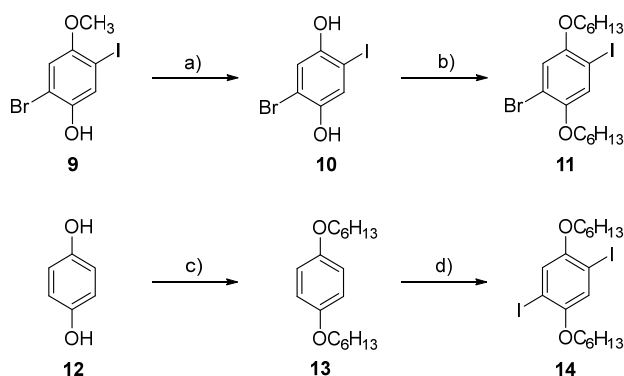
Ensemble absorption and PL spectra shown in Figure 2 (Main Text) were recorded by dissolving the analyte in toluene solution and filling this into a 10 mm quartz cuvette (Hellma Analytics- Quartz SUPRASIL). The data were recorded using a Perkin Elmer spectrometer

(Lambda 650) for absorption and a Horiba Jobin Yvon Fluoromax 4 for PL. Spectra were background corrected and normalized.

The PL decay of **1** in toluene solution was measured on an inverted confocal microscope as described elsewhere [S6]. A frequency-doubled Ti:sapphire oscillator (Spectra Physics Mai Tai BB) operating at 440 nm and 80 MHz repetition frequency was used for excitation. Using a single-photon counting module (Picoquant-MPD-050-CTB), we recorded the signal over a time period of 5 minutes. The extracted PL lifetimes shown in Figure 2b were confirmed by additional measurements using a picosecond streak-camera system (data not shown).

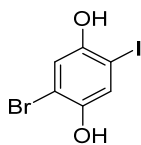
Single-molecule measurements were performed under excitation at a wavelength of 440 nm with a power density of approx.  $750 \text{ Wcm}^{-2}$  using two single photon detectors (Picoquant- $\pi$ -SPAD-20) in a Hanbury Brown and Twiss detection geometry.

## 2 Synthesis of halogenated hydroquinone dialkylethers



**Scheme S1.** Synthesis of halogenated hydroquinone dialkylethers. a)  $\text{BBr}_3$ ,  $\text{CH}_2\text{Cl}_2$ ,  $-78\text{ }^\circ\text{C}$  to rt, 16 h, quant.; b)  $\text{K}_2\text{CO}_3$ , 1-bromohexane, acetone, reflux, 48 h, 66 %; c)  $\text{K}_2\text{CO}_3$ , 1-iodohexane, acetone, reflux, 7 d, 63 %; d)  $\text{I}_2$ ,  $\text{KIO}_3$ ,  $\text{H}_2\text{SO}_4$ ,  $\text{AcOH}$ ,  $\text{CHCl}_3$ , reflux, 24 h, 47 %.

### 10



Under an Ar atmosphere, **9** (30.0 g, 0.09 mol) [S1] in  $\text{CH}_2\text{Cl}_2$  (200 mL) was cooled to  $-78\text{ }^\circ\text{C}$  and  $\text{BBr}_3$  (1 M in  $\text{CH}_2\text{Cl}_2$ , 273.0 mL, 0.273 mol) was slowly added. The solution was stirred for 16 h while it slowly warmed to rt. The suspension was poured onto ice, and ether was added. The aqueous phase was extracted with ether, and the combined organic phase was washed with water and brine and dried over  $\text{MgSO}_4$ . After evaporation of the solvent and recrystallization from *n*-heptane, **10** was obtained as a fawn solid (28.3 g, 0.09 mol, quant.).

**formula:**  $\text{C}_6\text{H}_4\text{O}_2\text{IBr}$ , **molar mass:** 314.90 g/mol.

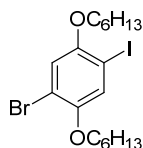
$^1\text{H NMR}$  (500 MHz,  $\text{DMSO}-d_6$ , rt)  $\delta$  [ppm]: 6.86 (s, 1H), 6.59 (s, 1H).

$^{13}\text{C NMR}$  (126 MHz,  $\text{DMSO}-d_6$ , rt)  $\delta$  [ppm]: 150.4, 147.9, 125.4, 118.3, 109.7, 83.6.

**MS** (EI, 70 eV)  $m/z$  (%): 313.8 (100)  $[\text{M}]^{+\bullet}$ , 235.9 (15)  $[\text{C}_6\text{H}_5\text{IO}_2]^+$ , 188.9 (20)  $[\text{C}_6\text{H}_4\text{BrO}_2]^+$ , 79.0 (20)  $[\text{C}_6\text{H}_7]^+$ , 53.0 (25)  $[\text{C}_4\text{H}_5]^+$ .

**calculated exact mass:** 313.84 g/mol.

## 11



**10** (20.0 g, 0.06 mol), K<sub>2</sub>CO<sub>3</sub> (43.9 g, 0.32 mol) and KI (0.53 g, 3.18 mmol) were suspended in acetone (300 mL). 1-Bromohexane (22.2 mL, 0.16 mol) was added, and the mixture was heated to reflux for 48 h. The solvent was removed and the residue treated with water and CH<sub>2</sub>Cl<sub>2</sub>. The aqueous phase was extracted with CH<sub>2</sub>Cl<sub>2</sub>, and the organic phase was washed with water and brine and dried over MgSO<sub>4</sub>. After evaporation of the solvent and recrystallization from methanol, **11** was obtained as a colorless solid (16.3 g, 0.03 mol, 66 %).

**formula:** C<sub>18</sub>H<sub>28</sub>BrIO<sub>2</sub>, **molar mass:** 483.23 g/mol.

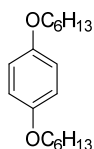
**<sup>1</sup>H NMR** (500 MHz, CDCl<sub>3</sub>, rt)  $\delta$  [ppm]: 7.28 (s, 1H), 6.98 (s, 1H), 3.94 (td, <sup>3</sup>J<sub>HH</sub> = 6.5 Hz, <sup>3</sup>J<sub>HH</sub> = 5.0 Hz, 4H), 1.84 – 1.76 (m, 4H), 1.56 – 1.44 (m, 4H), 1.38 – 1.30 (m, 8H), 0.95 – 0.87 (m, 6H).

**<sup>13</sup>C NMR** (126 MHz, CDCl<sub>3</sub>, rt)  $\delta$  [ppm]: 152.7, 150.6, 124.4, 117.3, 112.7, 84.9, 70.6, 70.5, 31.6, 31.6, 29.3, 29.24, 25.9, 25.8, 22.7, 14.2, 14.2.

**MS** (EI, 70 eV) *m/z* (%): 482.0 (30) [M]<sup>+</sup>, 397.9 (20) [C<sub>12</sub>H<sub>16</sub>BrIO<sub>2</sub>]<sup>+</sup>, 313.8 (100) [C<sub>6</sub>H<sub>4</sub>BrIO<sub>2</sub>]<sup>+</sup>, 235.9 (10) [C<sub>6</sub>H<sub>5</sub>IO<sub>2</sub>]<sup>+</sup>.

**calculated exact mass:** 482.03 g/mol.

## 13



Hydroquinone (**12**) (10.00 g, 90.82 mmol), K<sub>2</sub>CO<sub>3</sub> (62.76 g, 454.10 mmol), and 1-iodohexane (33.43 mL, 227.05 mmol) in acetone (300 mL) were refluxed for 7 d. The solvent was removed, and the residue was treated with water and CH<sub>2</sub>Cl<sub>2</sub>. The aqueous phase was extracted with CH<sub>2</sub>Cl<sub>2</sub>, and the organic phase was washed with water and brine and dried over MgSO<sub>4</sub>. After evaporation of the solvent and recrystallization from methanol, **13** was obtained as a colorless solid (15.93 g, 57.22 mmol, 63 %).

**formula:** C<sub>18</sub>H<sub>30</sub>O<sub>2</sub>, **molar mass:** 278.44 g/mol.

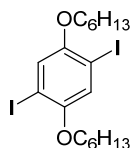
**<sup>1</sup>H NMR** (500 MHz, CDCl<sub>3</sub>, rt) δ [ppm]: 6.82 (s, 4H), 3.90 (t, <sup>3</sup>J<sub>HH</sub> = 6.6 Hz, 4H), 1.80 – 1.70 (m, 4H), 1.50 – 1.39 (m, 4H), 1.39 – 1.28 (m, 8H), 0.94 – 0.85 (m, 6H).

**<sup>13</sup>C NMR** (126 MHz, CDCl<sub>3</sub>, rt) δ [ppm]: 153.4, 115.6, 68.8, 31.8, 29.5, 25.9, 22.8, 14.2.

**MS** (EI, 70 eV) *m/z* (%): 278.2 (28) [M]<sup>+</sup>, 194.0 (20) [C<sub>12</sub>H<sub>18</sub>O<sub>2</sub>]<sup>+</sup>, 109.9 (100) [C<sub>6</sub>H<sub>5</sub>O<sub>2</sub>]<sup>+</sup>.

**calculated exact mass:** 278.22 g/mol.

## 14



**13** (14.82 g, 0.05 mol), I<sub>2</sub> (16.24 g, 0.06 mmol), KIO<sub>3</sub> (7.94 g, 0.04 mol), water (5 mL), H<sub>2</sub>SO<sub>4</sub> (conc., 6 mL), acetic acid (100 mL), and CHCl<sub>3</sub> (50 mL) were refluxed for 24 h. After cooling to rt, an aqueous Na<sub>2</sub>SO<sub>3</sub> solution (40 wt%), an aqueous NaOH solution (10 wt%), and CH<sub>2</sub>Cl<sub>2</sub> were slowly added. The aqueous phase was extracted with CH<sub>2</sub>Cl<sub>2</sub>, and the organic phase was washed with aqueous NaOH solution (10 wt%), water, and brine and dried over MgSO<sub>4</sub>. After evaporation of the solvent and recrystallization from ethanol, **14** was obtained as a slightly pink solid (13.21 g, 0.02 mol, 47 %).

**formula:** C<sub>18</sub>H<sub>28</sub>O<sub>2</sub>I<sub>2</sub>, **molar mass:** 530.23 g/mol.

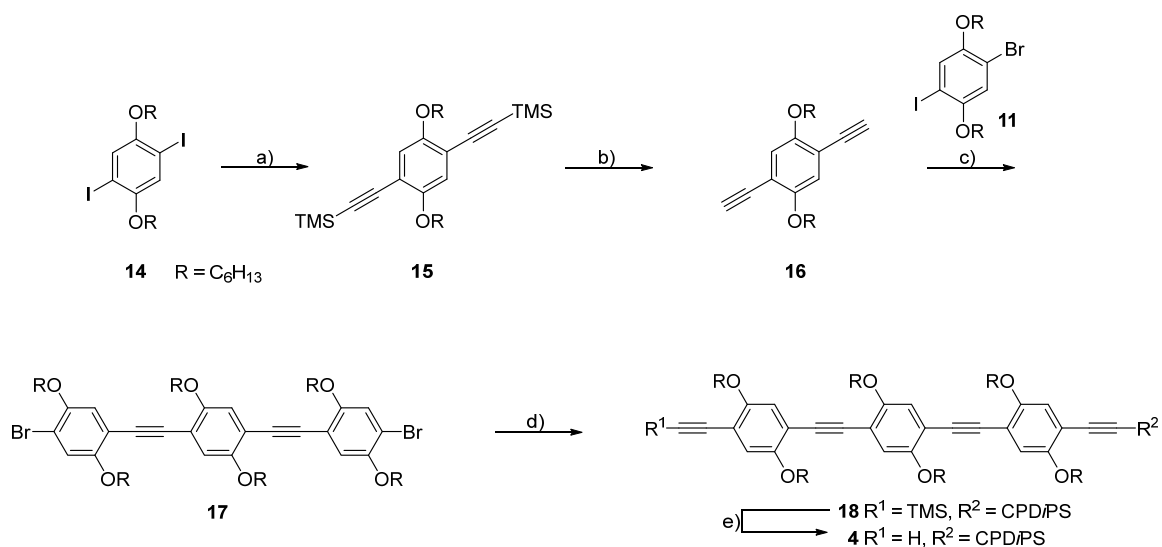
**<sup>1</sup>H NMR** (500 MHz, CDCl<sub>3</sub>, rt) δ [ppm]: 7.17 (s, 2H), 3.93 (t, <sup>3</sup>J<sub>HH</sub> = 6.4 Hz, 4H), 1.83 – 1.76 (m, 4H), 1.54 – 1.46 (m, 4H), 1.39 – 1.33 (m, 8H), 0.95 – 0.89 (m, 6H).

**<sup>13</sup>C NMR** (126 MHz, CDCl<sub>3</sub>, rt) δ [ppm]: 153.0, 123.0, 86.5, 70.5, 31.6, 29.3, 25.9, 22.7, 14.2.

**MS** (EI, 70 eV) *m/z* (%): 530.0 (40) [M]<sup>+</sup>, 445.9 (18) [C<sub>12</sub>H<sub>16</sub>I<sub>2</sub>O<sub>2</sub>]<sup>+</sup>, 361.8 (100) [C<sub>15</sub>H<sub>22</sub>I<sub>2</sub>O<sub>2</sub>]<sup>+</sup>.

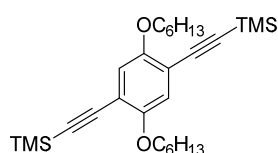
**calculated exact mass:** 530.02 g/mol.

### 3 Synthesis of 4



**Scheme S2.** a)  $Pd(PPh_3)_2Cl_2$ ,  $PPh_3$ ,  $CuI$ , piperidine, THF, 40 °C, 16 h, 82 %; b)  $K_2CO_3$ , MeOH, THF, rt, 16 h, 92 %; c)  $Pd(PPh_3)_2Cl_2$ ,  $PPh_3$ ,  $CuI$ ,  $NEt_3$ , THF, rt, 16 h, 75 %; d) 1)  $Pd(PPh_3)_2Cl_2$ ,  $PPh_3$ ,  $CuI$ , piperidine, THF, CPD/PS-acetylene, 50 °C, 16 h; 2) TMS-acetylene, 50 °C, 16 h, 41 %; e)  $K_2CO_3$ , MeOH, THF, rt, 2 h, 87 %.

### 15



Under an Ar atmosphere, **11** (16.6 g, 20.0 mmol) in THF (30 mL) and piperidine (80 mL) was purged with Ar for 30 min.  $Pd(PPh_3)_2Cl_2$  (0.14 g, 0.2 mmol),  $PPh_3$  (0.32 g, 1.2 mmol),  $CuI$  (0.15 g, 0.8 mmol), and TMS-acetylene (9.82 g, 0.1 mol) were added, and the mixture was stirred at 40 °C for 16 h. After cooling to rt, water and  $CH_2Cl_2$  were added. The aqueous phase was extracted with  $CH_2Cl_2$ , and the organic phase was washed with an aqueous  $H_2SO_4$  solution (10 wt%), water, and brine and dried over  $MgSO_4$ . After evaporation of the solvent, column chromatographic purification (Cy:DCM = 5:1,  $R_f = 0.38$ ) gave **16** as a slightly yellow solid (7.71 g, 16.39 mmol, 82 %).

**formula:**  $C_{28}H_{46}O_2Si_2$ , **molar mass:** 470.84 g/mol.

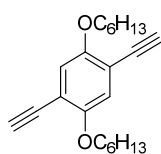
$^1H$  NMR (500 MHz,  $CDCl_3$ , rt)  $\delta$  [ppm]: 6.89 (s, 2H), 3.94 (t,  $^3J_{HH} = 6.4$  Hz, 4H), 1.83 – 1.73 (m, 4H), 1.52 – 1.47 (m, 4H), 1.36 – 1.30 (m, 8H), 0.95 – 0.86 (m, 6H), 0.25 (s, 18H).

**$^{13}\text{C}$  NMR** (126 MHz,  $\text{CDCl}_3$ , rt)  $\delta$  [ppm]: 154.2, 117.4, 114.1, 101.2, 100.2, 69.6, 31.8, 29.4, 25.8, 22.8, 14.2, 1.2, 0.1.

**MS** (EI, 70 eV)  $m/z$  (%): 470.4 (100)  $[\text{M}]^{+\bullet}$ , 386.3  $[\text{C}_{22}\text{H}_{34}\text{O}_2\text{Si}_2]^+$ , 302.2  $[\text{C}_{16}\text{H}_{22}\text{O}_2\text{Si}_2]^+$ , 287.1  $[\text{C}_{15}\text{H}_{19}\text{O}_2\text{Si}_2]^+$ .

**calculated exact mass:** 470.30 g/mol.

## 16



**15** (7.7 g, 16.4 mmol) in THF (160 mL) and MeOH (65 mL) was purged with Ar for 1 h.  $\text{K}_2\text{CO}_3$  (24.9 g, 0.18 mol) was added, and the mixture was stirred for 16 h. Water and  $\text{CH}_2\text{Cl}_2$  were added, the aqueous phase was extracted with  $\text{CH}_2\text{Cl}_2$ , and the combined organic phase was washed with water and brine and dried over  $\text{MgSO}_4$ . After evaporation of the solvent, column chromatographic purification (Cy:DCM = 5:1,  $R_f$  = 0.23) gave **16** as a slightly yellow solid (4.91 g, 15.05 mmol, 92 %).

**formula:**  $\text{C}_{22}\text{H}_{30}\text{O}_2$ , **molar mass:** 326.48 g/mol.

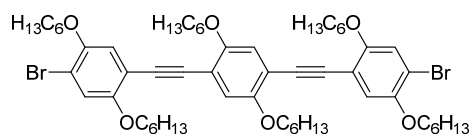
**$^1\text{H}$  NMR** (500 MHz,  $\text{CDCl}_3$ , rt)  $\delta$  [ppm]: 6.95 (s, 2H), 3.97 (t,  $^3J_{\text{HH}}$  = 6.6 Hz, 4H), 3.33 (s, 2H), 1.83 – 1.76 (m, 4H), 1.51 – 1.43 (m, 4H), 1.38 – 1.29 (m, 8H), 0.92 – 0.87 (m, 6H).

**$^{13}\text{C}$  NMR** (126 MHz,  $\text{CDCl}_3$ , rt)  $\delta$  [ppm]: 154.1, 117.9, 113.4, 82.5, 79.9, 69.8, 31.7, 29.2, 25.7, 22.7, 14.2.

**MS** (EI, 70 eV)  $m/z$  (%): 326.2 (35)  $[\text{M}]^{+\bullet}$ , 242.1 (15)  $[\text{C}_{16}\text{H}_{18}\text{O}_2]^+$ , 158.0 (100)  $[\text{C}_{10}\text{H}_6\text{O}_2]^+$ .

**calculated exact mass:** 326.22 g/mol.

## 17



**16** (4.1 g, 12.4 mmol) and **11** (13.8 g, 28.5 mmol) in THF (70 mL) were purged with Ar for 30 min. Pd(PPh<sub>3</sub>)<sub>2</sub>Cl<sub>2</sub> (0.26 g, 0.37 mmol), PPh<sub>3</sub> (0.29 g, 1.2 mmol), CuI (0.24 g, 0.8 mmol), and NEt<sub>3</sub> (35 mL) were added and the mixture stirred at rt for 16 h. Water and CH<sub>2</sub>Cl<sub>2</sub> were added, the aqueous phase was extracted with CH<sub>2</sub>Cl<sub>2</sub>, and the organic phase was washed with aqueous H<sub>2</sub>SO<sub>4</sub>-solution (10 wt%), water and brine and dried over MgSO<sub>4</sub>. After evaporation of the solvent, column chromatographic purification (Cy:DCM = 2:1 → 3:2, R<sub>f</sub> = 0.36 (2:1)) gave **17** as a slightly yellow solid (9.59 g, 9.25 mmol, 75 %).

**formula:** C<sub>58</sub>H<sub>84</sub>Br<sub>2</sub>O<sub>6</sub>, **molar mass:** 1037.11 g/mol.

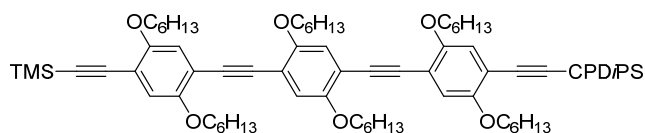
**<sup>1</sup>H NMR** (500 MHz, CDCl<sub>3</sub>, rt) δ [ppm]: 7.10 (s, 2H), 7.01 (s, 2H), 7.00 (s, 2H), 4.05 – 3.94 (m, 12H), 1.90 – 1.76 (m, 12H), 1.55 – 1.45 (m, 12H), 1.38 – 1.28 (m, 24H), 0.93 – 0.85 (m, 18H).

**<sup>13</sup>C NMR** (126 MHz, CDCl<sub>3</sub>, rt) δ [ppm]: 154.2, 153.6, 149.6, 118.3, 117.9, 117.4, 114.4, 113.5, 113.1, 91.0, 90.7, 70.2, 70.1, 69.8, 31.8, 31.7, 31.7, 29.4, 29.4, 29.3, 25.8, 25.8, 25.8, 22.8, 22.8, 22.7, 14.2.

**MS** (MALDI-TOF, DCTB) *m/z*: 1036.5 [M]<sup>+</sup>.

**calculated exact mass:** 1034.46 g/mol.

## 18



Under an Ar atmosphere, Pd(PPh<sub>3</sub>)<sub>2</sub>Cl<sub>2</sub> (55.7 mg, 0.08 mmol), PPh<sub>3</sub> (10.4 mg, 0.04 mmol), CuI (7.6 mg, 0.04 mmol) and CPDiPS-acetylene (180.9 mg, 0.87 mmol) [S2] were added to a solution of **17** (822.3 mg, 793 μmol) in THF (5 mL) and piperidine (15 mL), and the mixture was stirred at 50 °C for 16 h. Then, TMS-acetylene (0.45 mL, 3.17 mmol) was added, and the mixture was additionally stirred at 50 °C for 16 h. After cooling to rt, water and CH<sub>2</sub>Cl<sub>2</sub> were added. The aqueous phase was extracted with CH<sub>2</sub>Cl<sub>2</sub>, and the organic phase was washed with aqueous HCl (2 M), water and brine and dried over MgSO<sub>4</sub>. After evaporation of the solvent,

column chromatographic purification (Cy:DCM = 1:1,  $R_f$  = 0.63) gave **18** as a slightly yellow solid (383.9 mg, 325  $\mu$ mol, 41 %).

**formula:**  $C_{75}H_{113}NO_6Si_2$ , **molar mass:** 1180.90 g/mol.

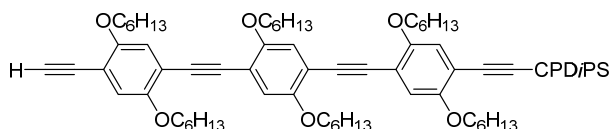
$^1H$  NMR (500 MHz,  $CDCl_3$ , rt)  $\delta$  [ppm]: 7.00 (s, 1H), 6.99 (s, 1H), 6.96 (s, 1H), 6.95 (s, 1H), 6.94 (s, 1H), 6.93 (s, 1H), 4.05 – 3.93 (m, 12H), 2.43 (t,  $^3J_{HH}$  = 7.0 Hz, 2H), 1.92 – 1.75 (m, 14H), 1.56 – 1.45 (m, 12H), 1.39 – 1.30 (m, 24H), 1.15 – 1.09 (m, 14H), 0.93 – 0.86 (m, 20H), 0.26 (s, 9H).

$^{13}C$  NMR (126 MHz,  $CDCl_3$ , rt)  $\delta$  [ppm]: 154.5, 154.3, 153.7, 153.5, 153.4, 119.9, 118.0, 117.6, 117.4, 117.4, 117.2, 116.6, 115.0, 114.7, 114.5, 114.4, 113.9, 113.4, 104.1, 101.3, 100.2, 95.3, 91.7, 91.7, 91.6, 91.6, 70.0, 69.8, 69.8, 69.6, 69.3, 31.8, 31.8, 31.8, 29.5, 29.5, 29.5, 29.4, 29.4, 29.4, 25.9, 25.9, 25.8, 25.8, 25.8, 22.8, 22.8, 21.5, 20.9, 18.4, 18.1, 14.2, 14.2, 12.0, 9.8.

**MS** (MALDI-TOF, DCTB)  $m/z$ : 1179.8 [M] $^+$ .

**calculated exact mass:** 1179.81 g/mol.

#### 4



**18** (222.7 mg, 189  $\mu$ mol) in THF (15 mL) and MeOH (5 mL) was purged with Ar for 1 h.  $K_2CO_3$  (261.2 mg, 1.89 mmol) was added, and the mixture was stirred for 3 h. Water and  $CH_2Cl_2$  were added, the aqueous phase was extracted with  $CH_2Cl_2$ , and the organic phase was washed with water and brine and dried over  $MgSO_4$ . After evaporation of the solvent, column chromatographic purification (Cy:DCM = 2:1  $\rightarrow$  3:2,  $R_f$  = 0.36 (2:1)) gave **4** as a yellow solid (183.3 mg, 165  $\mu$ mol, 87 %).

**formula:**  $C_{72}H_{105}NO_6Si$ , **molar mass:** 1108.72 g/mol.

$^1H$  NMR (500 MHz,  $CDCl_3$ , rt)  $\delta$  [ppm]: 7.00 (s, 1H), 7.00 (s, 1H), 6.99 (s, 1H), 6.97 (s, 1H), 6.95 (s, 1H), 6.93 (s, 1H), 4.05 – 3.98 (m, 10H), 3.95 (t,  $^3J_{HH}$  = 6.5 Hz, 2H), 3.34 (s, 1H), 2.43 (t,  $^3J_{HH}$  = 7.0 Hz, 2H), 1.93 – 1.74 (m, 14H), 1.56 – 1.45 (m, 12H), 1.38 – 1.27 (m, 24H), 1.15 – 1.06 (m, 14H), 0.93 – 0.81 (m, 20H).

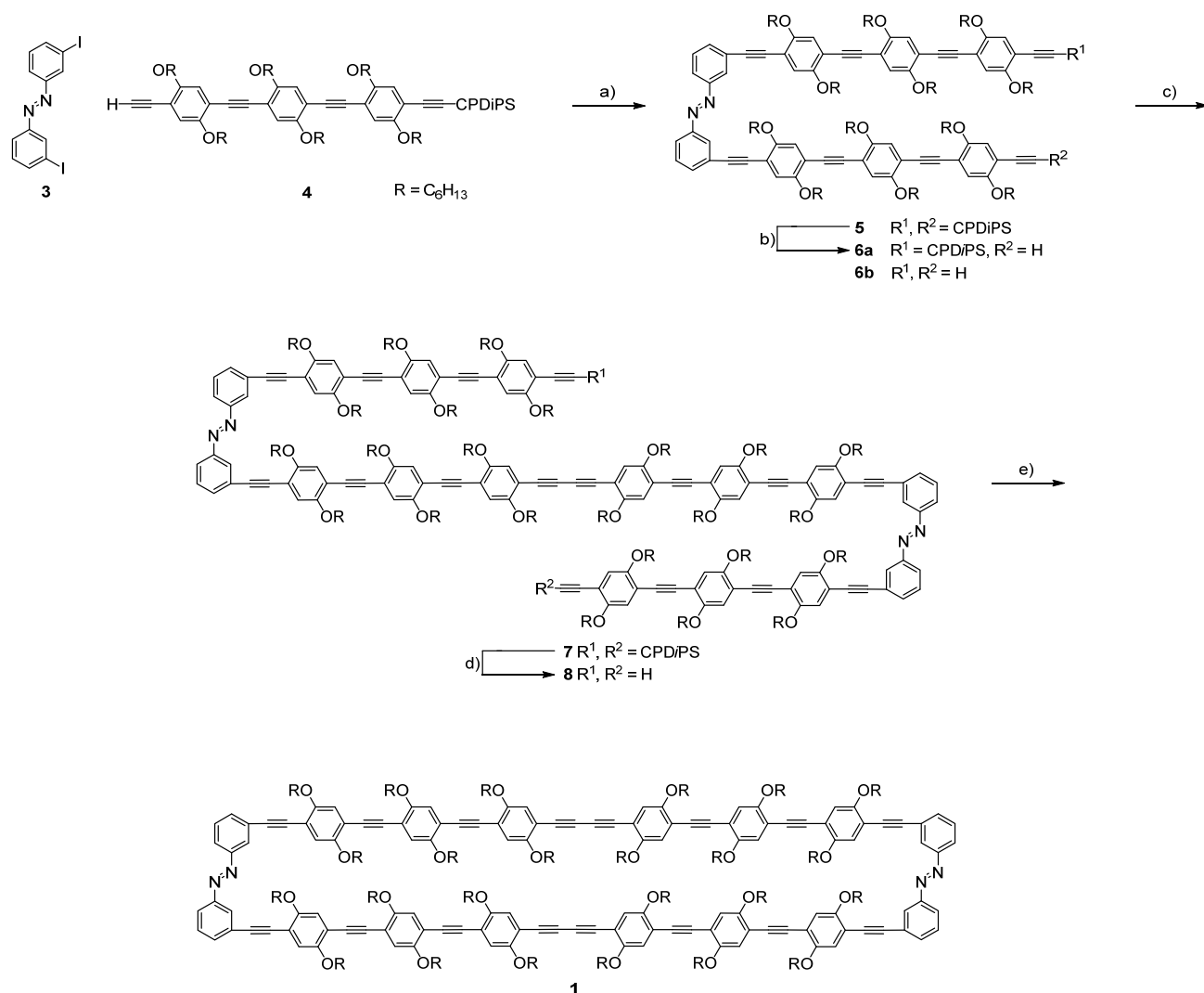
$^{13}C$  NMR (126 MHz,  $CDCl_3$ , rt)  $\delta$  [ppm]: 54.5, 154.3, 153.7, 153.7, 153.5, 153.4, 119.9, 118.1, 118.0, 117.4, 117.2, 116.6, 115.1, 115.0, 114.5, 114.4, 113.4, 112.7, 104.1, 95.3, 91.7, 91.6,

91.4, 82.4, 80.2, 70.0, 69.9, 69.8, 69.8, 69.3, 31.8, 31.8, 31.8, 31.7, 29.5, 29.5, 29.4, 29.3, 25.9, 25.8, 25.8, 25.8, 22.8, 22.8, 22.7, 21.5, 20.9, 18.4, 18.2, 14.2, 14.2, 14.2, 12.0, 9.8.

MS (MALDI-TOF, DCTB)  $m/z$ : 1107.8  $[M]^+$ .

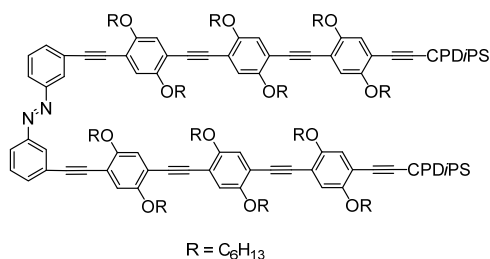
calculated exact mass: 1107.77 g/mol.

#### 4 Synthesis of 1



**Scheme S3.** a) Pd(PPh<sub>3</sub>)<sub>4</sub>, CuI, piperidine, THF, rt, 6 d, 71 %; b) TBAF (1 M in THF), THF, H<sub>2</sub>O (5 vol%), rt, 5 h, 32 %; c) Pd(PPh<sub>3</sub>)<sub>2</sub>Cl<sub>2</sub>, PPh<sub>3</sub>, I<sub>2</sub>, HN(*i*Pr)<sub>2</sub>, THF, rt, 16 h, 48 %; d) TBAF (1 M in THF), THF, rt, 12 h, 81 %; e) Pd(PPh<sub>3</sub>)<sub>2</sub>Cl<sub>2</sub>, CuI, I<sub>2</sub>, HN(*i*Pr)<sub>2</sub>, THF, 50 °C, 144 h, 50-60 %;

## 5



Under an Ar atmosphere, **3** (36.0 mg, 71  $\mu$ mol) [S3], **4** (200.0 mg, 0.18 mmol), Pd(PPh<sub>3</sub>)<sub>4</sub> (9.5 mg, 0.008 mmol), and CuI (1.0 mg, 0.004 mmol) in piperidine (15 mL) and THF (5 mL) were stirred at rt for 6 d. Water and CH<sub>2</sub>Cl<sub>2</sub> were added, the aqueous phase was extracted with CH<sub>2</sub>Cl<sub>2</sub>, and the organic phase was washed with aqueous HCl (2 M), water and brine and dried over MgSO<sub>4</sub>. After evaporation of the solvent, column chromatographic purification (Cy:DCM = 1:1  $\rightarrow$  2:3; *R<sub>f</sub>* = 0.53 (2:3)) gave **5** as a yellow film (139.8 mg, 58  $\mu$ mol, 71 %).

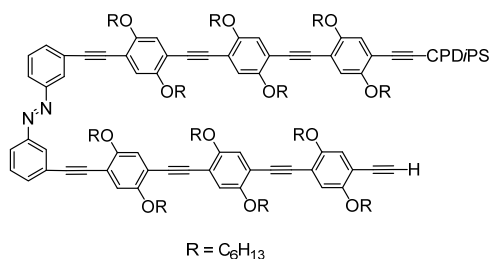
**formula:** C<sub>156</sub>H<sub>216</sub>N<sub>4</sub>O<sub>12</sub>Si<sub>2</sub>, **molar mass:** 2395.63 g/mol.

**<sup>1</sup>H NMR** (500 MHz, CDCl<sub>3</sub>, rt)  $\delta$  [ppm]: 8.10 (t, <sup>4</sup>*J*<sub>HH</sub> = 1.8 Hz, 2H), 7.91 (ddd, <sup>3</sup>*J*<sub>HH</sub> = 8.0 Hz, <sup>4</sup>*J*<sub>HH</sub> = 2.0 Hz, <sup>4</sup>*J*<sub>HH</sub> = 1.2 Hz, 2H), 7.65 (dt, <sup>3</sup>*J*<sub>HH</sub> = 7.7 Hz, <sup>4</sup>*J*<sub>HH</sub> = 1.3 Hz, 2H), 7.52 (t, <sup>3</sup>*J*<sub>HH</sub> = 7.8 Hz, 2H), 7.05 (s, 2H), 7.04 (s, 2H), 7.02 (s, 2H), 7.01 (s, 2H), 6.96 (s, 2H), 6.93 (s, 2H), 4.08 – 4.00 (m, 20H), 3.96 (t, <sup>3</sup>*J*<sub>HH</sub> = 6.4 Hz, 4H), 2.44 (t, <sup>3</sup>*J*<sub>HH</sub> = 7.0 Hz, 4H), 1.94 – 1.81 (m, 28H), 1.61 – 1.46 (m, 24H), 1.43 – 1.24 (m, 48H), 1.15 – 1.06 (m, 28H), 0.94 – 0.82 (m, 40H).

**<sup>13</sup>C NMR** (126 MHz, CDCl<sub>3</sub>, rt)  $\delta$  [ppm]: 154.5, 153.9, 153.7, 153.4, 152.5, 134.2, 129.3, 125.9, 124.7, 123.2, 119.9, 118.0, 117.4, 117.4, 117.3, 116.6, 115.0, 114.8, 114.5, 114.4, 113.8, 113.4, 104.1, 95.3, 94.2, 91.8, 91.8, 91.7, 91.6, 87.1, 70.0, 69.9, 69.9, 69.8, 69.3, 31.8, 31.8, 29.9, 29.6, 29.5, 29.5, 29.5, 27.1, 26.0, 26.0, 25.9, 25.8, 25.8, 22.8, 22.8, 21.5, 20.9, 18.4, 18.2, 14.2, 14.2, 12.0, 9.8, 1.2.

**MS** (MALDI-TOF, DCTB) *m/z*: 2393.6 [M]<sup>+</sup>, 2643.7 [M+DCTB]<sup>+</sup>.

**calculated exact mass:** 2393.60 g/mol.

**6a**

Under an Ar atmosphere, TBAF (1 M in THF, 0.1 mL, 0.1 mmol) was added to **5** (130.0 mg, 54  $\mu$ mol) in THF (6 mL) and water (0.24 mL). After 1 h, 1.5 h, and 2.5 h, additional portions of TBAF (each 0.1 mL, 0.1 mmol) were added. After a total reaction time of 5 h, water and CH<sub>2</sub>Cl<sub>2</sub> were added, the aqueous phase was extracted with CH<sub>2</sub>Cl<sub>2</sub>, and the organic phase was washed with water and brine and dried over MgSO<sub>4</sub>. After evaporation of the solvent, column chromatographic purification (Cy:DCM = 2:3  $\rightarrow$  1:2,  $R_f$  = 0.64 (1:2)) and additional purification by rec GPC gave **6a** as a yellow film (38.5 mg, 0.02 mmol, 32 %). In addition, **6b** was also obtained as a yellow film (32.5 mg, 16.0  $\mu$ mol, 29 %) (Cy:DCM = 2:3  $\rightarrow$  1:2,  $R_f$  = 0.70 (1:2)).

**formula:** C<sub>146</sub>H<sub>197</sub>N<sub>3</sub>O<sub>12</sub>Si, **molar mass:** 2214.28 g/mol.

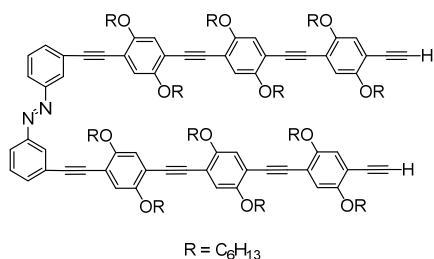
**<sup>1</sup>H NMR** (500 MHz, CDCl<sub>3</sub>, rt)  $\delta$  [ppm]: 8.10 (t, <sup>4</sup>J<sub>HH</sub> = 2.0 Hz, 2H), 7.92 – 7.89 (m, 2H), 7.65 (d, <sup>3</sup>J<sub>HH</sub> = 7.6 Hz, 2H), 7.52 (t, <sup>3</sup>J<sub>HH</sub> = 7.8 Hz, 2H), 7.07 – 6.91 (m, 12H), 4.10 – 3.93 (m, 24H), 3.34 (s, 1H), 2.44 (t, <sup>3</sup>J<sub>HH</sub> = 7.0 Hz, 2H), 1.94 – 1.75 (m, 26H), 1.62 – 1.42 (m, 24H), 1.42 – 1.28 (m, 48H), 1.16 – 1.04 (m, 14H), 0.94 – 0.81 (m, 38H).

**<sup>13</sup>C NMR** (126 MHz, CDCl<sub>3</sub>, rt)  $\delta$  [ppm]: 154.5, 154.3, 153.9, 153.7, 153.5, 153.4, 152.5, 134.2, 129.3, 125.9, 124.7, 123.2, 119.9, 118.1, 117.9, 117.4, 117.3, 117.2, 116.6, 114.8, 114.4, 113.8, 113.4, 112.7, 104.1, 95.3, 94.2, 91.7, 91.7, 91.4, 87.1, 82.4, 80.2, 70.0, 69.9, 69.8, 69.8, 69.8, 69.7, 69.3, 31.8, 31.8, 31.8, 31.7, 29.9, 29.5, 29.5, 29.5, 29.4, 29.4, 29.4, 29.3, 26.0, 25.9, 25.9, 25.8, 25.8, 25.8, 25.8, 22.8, 22.8, 22.7, 21.5, 20.9, 18.4, 18.2, 14.2, 14.2, 14.2, 12.0, 9.8.

**MS** (MALDI-TOF, DCTB)  $m/z$ : 2212.4 [M]<sup>+</sup>, 2462.5 [M+DCTB]<sup>+</sup>.

**calculated exact mass:** 2212.47 g/mol.

6b



**formula:** C<sub>136</sub>H<sub>178</sub>N<sub>2</sub>O<sub>12</sub>, **molar mass:** 2032.92 g/mol.

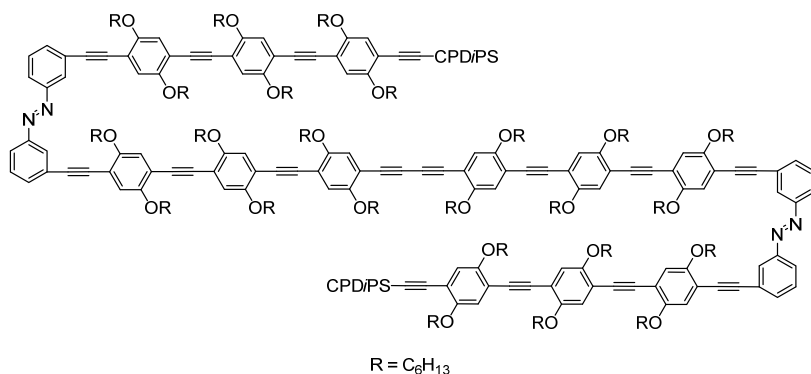
**<sup>1</sup>H NMR** (500 MHz, CDCl<sub>3</sub>, rt)  $\delta$  [ppm]: 8.10 (t, <sup>4</sup>J<sub>HH</sub> = 1.9 Hz, 2H), 7.91 (dt, <sup>3</sup>J<sub>HH</sub> = 8.0 Hz, <sup>4</sup>J<sub>HH</sub> = 1.6 Hz, 2H), 7.65 (dt, <sup>3</sup>J<sub>HH</sub> = 7.7 Hz, <sup>4</sup>J<sub>HH</sub> = 1.5 Hz, 2H), 7.52 (t, <sup>3</sup>J<sub>HH</sub> = 7.8 Hz, 2H), 7.05 (s, 1H), 7.04 (s, 1H), 7.02 (s, 1H), 7.01 (s, 1H), 7.00 (s, 1H), 6.98 (s, 1H), 4.09 – 3.98 (m, 24H), 3.34 (s, 2H), 1.91 – 1.79 (m, 24H), 1.61 – 1.46 (m, 24H), 1.43 – 1.30 (m, 24H), 1.30 – 1.17 (m, 24H), 0.94 – 0.82 (m, 36H).

**<sup>13</sup>C NMR** (126 MHz, CDCl<sub>3</sub>, rt)  $\delta$  [ppm]: 154.3, 153.9, 153.7, 153.7, 153.5, 152.5, 134.2, 129.3, 125.9, 124.7, 123.2, 118.1, 117.4, 117.3, 117.2, 115.1, 114.8, 114.5, 114.4, 113.8, 112.7, 94.2, 91.8, 91.7, 91.7, 91.4, 87.1, 82.4, 80.2, 69.9, 69.9, 69.8, 69.8, 69.8, 32.1, 31.8, 31.8, 31.8, 31.7, 29.9, 29.5, 29.5, 29.5, 29.4, 29.4, 29.3, 26.0, 25.8, 25.8, 25.8, 25.8, 22.8, 22.8, 22.8, 22.7, 14.3, 14.2, 14.2, 14.2.

**MS** (MALDI-TOF, DCTB)  $m/z$ : 2031.3 [M]<sup>+</sup>, 2281.4 [M+DCTB]<sup>+</sup>.

**calculated exact mass:** 2031.34 g/mol.

## 7



Under an Ar atmosphere, **6a** (78.5 mg, 36  $\mu$ mol), Pd(PPh<sub>3</sub>)<sub>2</sub>Cl<sub>2</sub> (7.5 mg, 0.01 mmol), CuI (5.1 mg, 0.03 mmol), and I<sub>2</sub> (16.2 mg, 0.06 mmol) in HN(*i*Pr)<sub>2</sub> (5 mL) and THF (7 mL) were stirred at rt for 16 h. Water and CH<sub>2</sub>Cl<sub>2</sub> were added, the aqueous phase was extracted with CH<sub>2</sub>Cl<sub>2</sub>, and the organic phase was washed with aqueous HCl (1 M), water, and brine and dried over MgSO<sub>4</sub>. After evaporation of the solvent, column chromatographic purification (Cy:DCM = 2:3  $\rightarrow$  1:2, R<sub>f</sub> = 0.45 (1:2)) and additional purification by rec GPC gave **7** as an orange film (37.7 mg, 8.5  $\mu$ mol, 48 %).

**formula:** C<sub>292</sub>H<sub>392</sub>N<sub>6</sub>O<sub>24</sub>Si<sub>2</sub>, **molar mass:** 4426.54 g/mol.

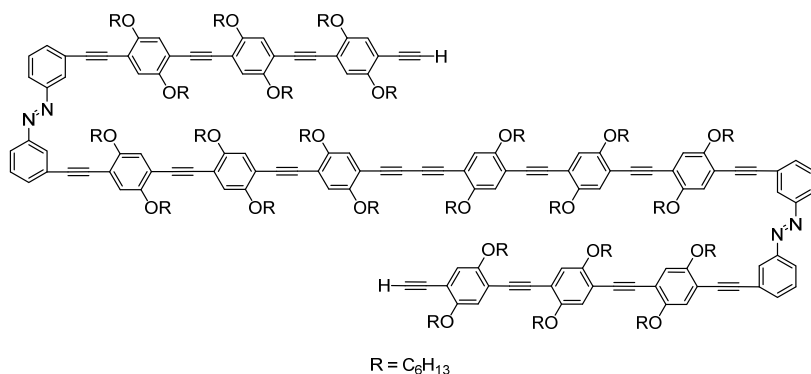
**<sup>1</sup>H NMR** (500 MHz, CDCl<sub>3</sub>, rt)  $\delta$  [ppm]: 8.10 (s, 4H), 7.91 (d, <sup>3</sup>J<sub>HH</sub> = 8.0 Hz, 4H), 7.65 (d, <sup>3</sup>J<sub>HH</sub> = 7.6 Hz, 4H), 7.52 (t, <sup>3</sup>J<sub>HH</sub> = 7.8 Hz, 4H), 7.06 – 6.92 (m, 24H), 4.09 – 3.94 (m, 48H), 2.43 (t, <sup>3</sup>J<sub>HH</sub> = 6.9 Hz, 4H), 1.92 – 1.76 (m, 52H), 1.62 – 1.46 (m, 48H), 1.41 – 1.28 (m, 96H), 1.16 – 1.07 (m, 28H), 0.95 – 0.80 (m, 76H).

**<sup>13</sup>C NMR** (126 MHz, CDCl<sub>3</sub>, rt)  $\delta$  [ppm]: 155.2, 154.5, 153.9, 153.7, 153.7, 153.5, 153.4, 152.6, 134.2, 129.3, 125.9, 125.7, 124.7, 123.2, 120.0, 118.0, 118.0, 117.4, 117.3, 117.3, 116.6, 115.6, 115.0, 114.8, 114.5, 114.4, 113.8, 113.4, 95.3, 94.2, 91.8, 91.8, 87.1, 70.0, 69.9, 69.9, 69.8, 69.3, 32.8, 32.1, 31.8, 31.8, 31.8, 31.7, 30.5, 29.9, 29.5, 29.5, 29.5, 29.4, 29.4, 29.3, 26.0, 26.0, 26.0, 25.8, 25.8, 25.8, 22.8, 22.8, 21.5, 20.9, 18.4, 18.2, 14.2, 12.0, 9.8, 1.2.

**MS** (MALDI-TOF, DCTB) *m/z*: 4422.9 [M]<sup>+</sup>, 4673.1 [M+DCTB]<sup>+</sup>, 4923.2 [M+2DCTB]<sup>+</sup>.

**calculated exact mass:** 4422.92 g/mol.

8



Under an Ar atmosphere, TBAF (1 M in THF, 0.07 mL, 0.07 mmol) was added to **7** (50.0 mg, 11  $\mu$ mol) in THF (7 mL) and stirred at rt for 12 h. Water and CH<sub>2</sub>Cl<sub>2</sub> were added, the aqueous phase was extracted with CH<sub>2</sub>Cl<sub>2</sub>, and the organic phase was washed with water and brine and dried over MgSO<sub>4</sub>. After evaporation of the solvent, column chromatographic purification (Cy:DCM = 1:1, *R<sub>f</sub>* = 0.58) and additional purification by rec GPC gave **7** as a yellow film (37 mg, 9  $\mu$ mol, 81 %).

**formula:** C<sub>272</sub>H<sub>354</sub>N<sub>4</sub>O<sub>24</sub>, **molar mass:** 4063.83 g/mol.

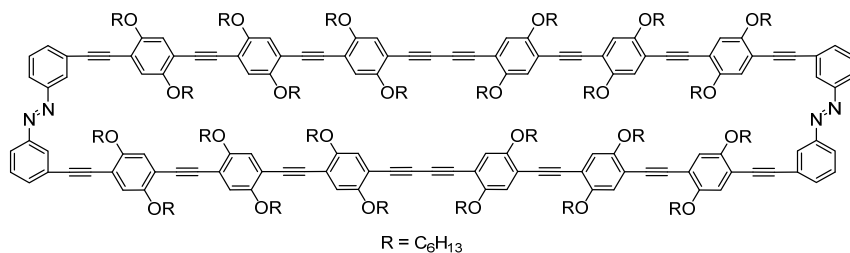
**<sup>1</sup>H NMR** (500 MHz, CDCl<sub>3</sub>, rt)  $\delta$  [ppm]: 8.11 – 8.09 (m, 4H), 7.94 – 7.88 (m, 4H), 7.67 – 7.64 (m, 4H), 7.52 (t, <sup>3</sup>*J*<sub>HH</sub> = 7.8 Hz, 4H), 7.06 – 6.97 (m, 24H), 4.09 – 3.98 (m, 48H), 3.34 (s, 2H), 1.92 – 1.77 (m, 48H), 1.61 – 1.46 (m, 48H), 1.42 – 1.29 (m, 96H), 0.96 – 0.85 (m, 72H).

**<sup>13</sup>C NMR** (126 MHz, CDCl<sub>3</sub>, rt)  $\delta$  [ppm]: 155.1, 154.3, 153.9, 153.7, 153.7, 153.7, 153.5, 153.5, 153.3, 152.5, 134.2, 130.9, 129.3, 128.8, 125.9, 124.7, 124.3, 123.2, 118.1, 118.0, 117.4, 117.3, 117.2, 117.2, 115.6, 115.1, 114.8, 114.6, 114.5, 114.4, 114.3, 113.8, 112.7, 94.2, 92.4, 91.8, 91.7, 91.7, 91.5, 91.4, 87.1, 82.4, 80.2, 79.8, 79.5, 69.9, 69.9, 69.8, 69.8, 69.8, 69.8, 69.7, 31.8, 31.8, 31.8, 31.7, 31.7, 29.5, 29.5, 29.4, 29.4, 29.4, 29.3, 29.3, 26.0, 25.8, 25.8, 25.8, 25.8, 25.8, 22.8, 22.8, 22.7, 14.2, 14.2, 1.2.

**MS** (MALDI-TOF, DCTB) *m/z*: 4060.7 [M]<sup>+</sup>, 4310.8 [M+DCTB]<sup>+</sup>, 4561.0 [M+2DCTB]<sup>+</sup>.

**calculated exact mass:** 4060.66 g/mol.

**1**



Under an Ar atmosphere, **8** (10.0 mg, 2.5  $\mu\text{mol}$ ) in THF (20 mL) was purged with Ar for 1 h. By using a syringe pump, this solution was slowly added (72 h) to Pd(PPh<sub>3</sub>)<sub>2</sub>Cl<sub>2</sub> (17.3 mg, 24.6  $\mu\text{mol}$ ), CuI (2.3 mg, 12.3  $\mu\text{mol}$ ), and I<sub>2</sub> (3.5 mg, 13.8  $\mu\text{mol}$ ) in THF (20 mL) and HN(*i*Pr)<sub>2</sub> (15 mL) at 50 °C and then additionally stirred for 72 h. After cooling to rt, water and CH<sub>2</sub>Cl<sub>2</sub> were added, the aqueous phase was extracted with CH<sub>2</sub>Cl<sub>2</sub>, and the organic phase was washed with water and brine and dried over MgSO<sub>4</sub>. After evaporation of the solvent, the crude product was dissolved in CH<sub>2</sub>Cl<sub>2</sub>, filtered through a plug of silica and purified by rec GPC to give **1** as a yellow film (5 – 6 mg, 1.23 – 1.48  $\mu\text{mol}$ , 50 – 60 %; variable yields of different reactions).

**formula:** C<sub>272</sub>H<sub>352</sub>N<sub>4</sub>O<sub>24</sub>, **molar mass:** 4061.81 g/mol.

**<sup>1</sup>H NMR** (700 MHz, CDCl<sub>3</sub>, rt)  $\delta$  [ppm]: 8.18 (d, <sup>4</sup>J<sub>HH</sub> = 1.9 Hz, 4H), 7.94 (dt, <sup>3</sup>J<sub>HH</sub> = 8.1 Hz, <sup>4</sup>J<sub>HH</sub> = 1.4 Hz, 4H), 7.63 (dt, <sup>3</sup>J<sub>HH</sub> = 7.5 Hz, <sup>4</sup>J<sub>HH</sub> = 1.3 Hz, 4H), 7.52 (t, <sup>3</sup>J<sub>HH</sub> = 7.7 Hz, 4H), 7.05 (s, 4H), 7.04 (s, 4H), 7.02 (s, 4H), 7.01 (s, 4H), 6.99 (s, 4H), 6.99 (s, 4H), 4.08 – 3.96 (m, 48H), 1.89 – 1.75 (m, 48H), 1.59 – 1.46 (m, 48H), 1.44 – 1.26 (m, 96H), 0.94 – 0.80 (m, 72H).

**<sup>13</sup>C NMR** (176 MHz, CDCl<sub>3</sub>, rt)  $\delta$  [ppm]: 155.1, 153.9, 153.7, 153.7, 153.7, 153.5, 152.3, 129.3, 124.8, 118.0, 117.4, 117.3, 117.3, 115.6, 114.8, 114.6, 114.4, 113.9, 112.7, 94.2, 92.5, 92.2, 91.6, 79.6, 69.9, 69.9, 69.9, 69.8, 45.4, 32.8, 31.8, 31.8, 31.7, 31.7, 31.2, 29.9, 29.5, 29.5, 29.4, 29.4, 29.4, 29.3, 26.7, 25.9, 25.9, 25.8, 25.8, 25.8, 25.8, 22.8, 22.8, 22.8, 22.7, 14.2, 14.2, 14.1, 14.1, 1.2.

**MS** (MALDI-TOF, DCTB)  $m/z$ : 4058.7 [M]<sup>+</sup>, 4308.8 [M+DCTB]<sup>+</sup>.

**calculated exact mass:** 4058.64 g/mol.

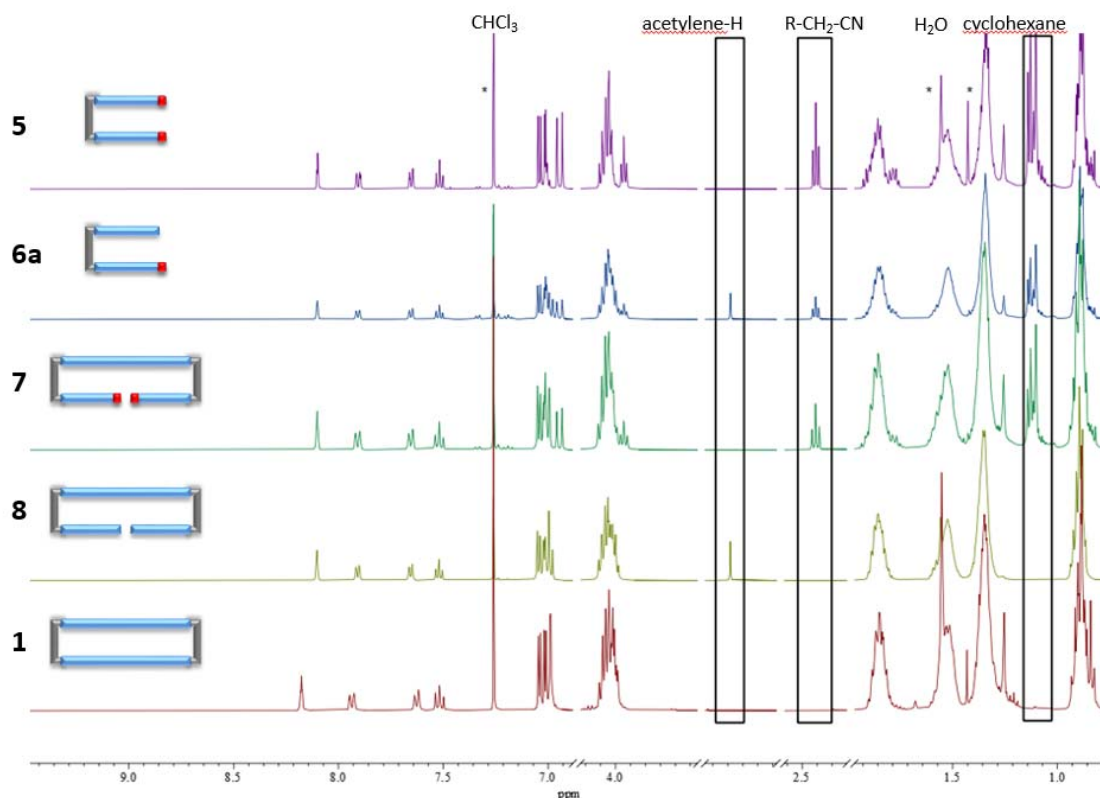


**Fig S1:**  $^1\text{H}$  NMR spectra of **5**, **6a**, **7**, **8**, and **1** (in  $\text{CDCl}_3$ , rt). Vanishing of the respective CPDiPS (right box) and acetylene (left box) signals show the progress of the deprotection and coupling reactions. While **5** – **8** show variable amounts of signals in the region of 6.6 ppm and 7.1 – 7.4 ppm (due to the presence of *cis* isomers), **1** does not contain any of these isomers in the NMR spectrum, even after irradiation. Signals marked with an asterisk belong to residual solvents ( $\text{CHCl}_3$ : 7.26 ppm;  $\text{H}_2\text{O}$ : 1.56 ppm. cyclohexane: 1.43 ppm).

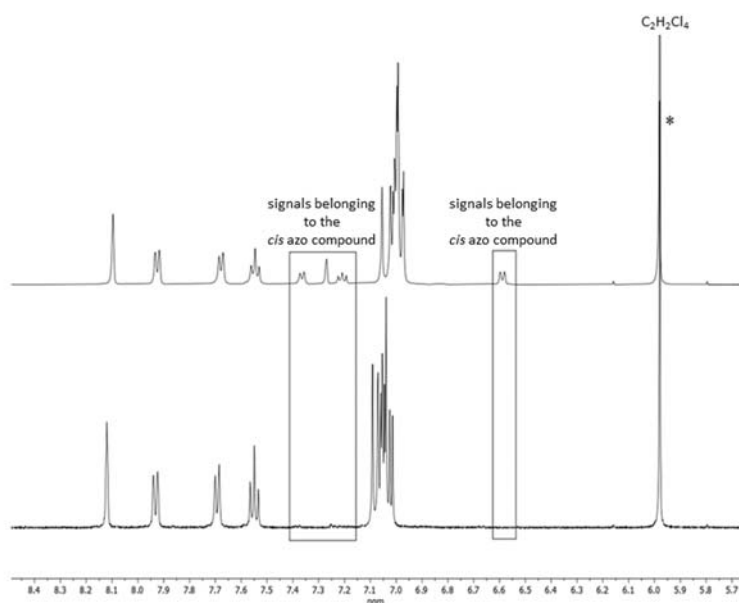


**Fig S2:**  $^1\text{H}$  NMR spectra (500 MHz) of **8** in  $\text{C}_2\text{D}_2\text{Cl}_4$  (residual protons at 5.91 ppm) at rt (top) and at 100 °C (bottom). At higher temperature, the solution contains exclusively the *trans* isomer.

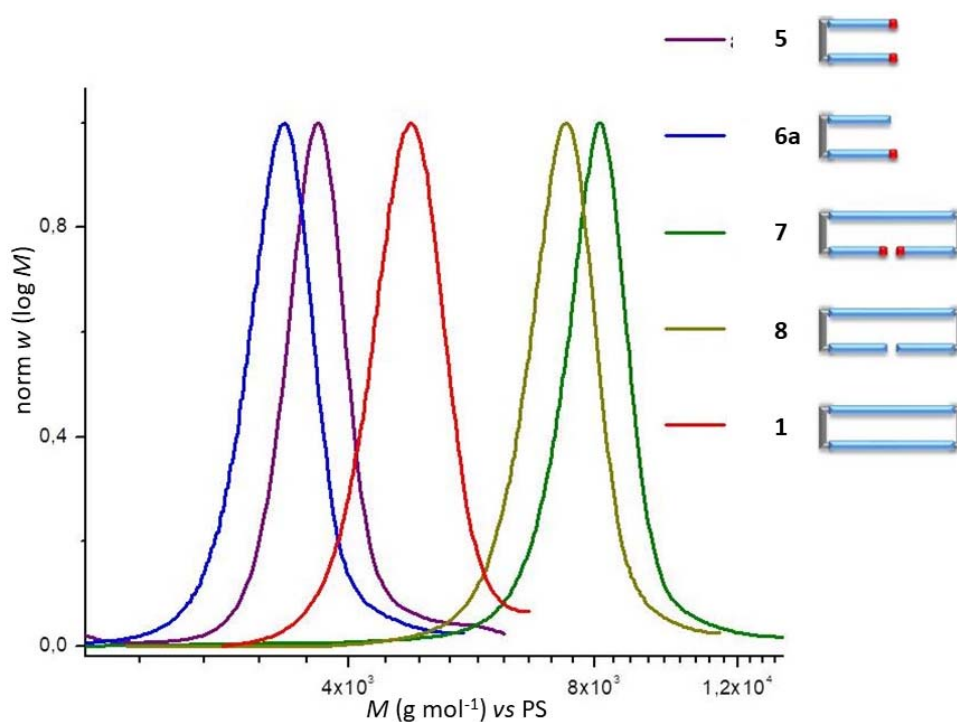


**Fig S3:** GPC elugrams of **5**, **6a**, **7**, **8**, and **1** (THF, rt, vs. polystyrene). As expected, the hydrodynamic radius dramatically decreases after the cyclization (**8** to **1**) suggesting a considerably lower molecular weight when the PS calibration is used for the molecular weight determination.

## 5 Additional molecular models and scanning tunneling microscopy images of **1** and **8**

Figures S4a and b as well as c and d show two limiting cases of the initially expected conformations of **1**:

- Figures S4a and b show a conformer in which a maximum of 12 side chains interdigitate in the intrannular nanopore. It is widened by deformation of the otherwise linear rigid rod units to have a maximum rod–rod distance of  $w_1$  of 1.6 nm. (Note that extraannular side-chains are not considered in the calculation, and are not shown here.)
- Additionally, Figures S4c and d show another conformer in which the rigid rod units are hardly bent and have a rod–rod distance of  $w_2 = 0.8$  nm, so that no side chains may adsorb in the intraannular lumen. (Note that extraannular side-chains and side-chains pointing towards the solution phase are not considered in the calculation, and are not shown in this model.)

In both cases, we obtained conformers in which all *p*-phenylene units are oriented coplanar to the underlying graphene substrate, similarly to the descriptions in *e.g.* Ref. [S4]. (Note that this does not necessarily apply to sterically constrained structures and has been explicitly described for systems with highly strained backbones.[S5])

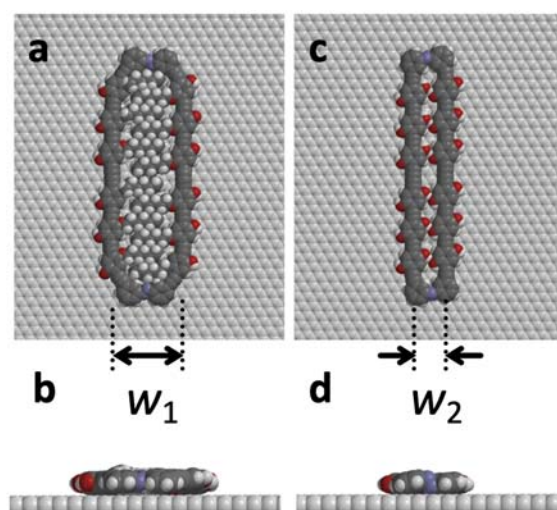


**Figure S4:** (a) – (d) Space-filling models of (*trans/trans*)-**1**, having rod–rod widths of (a) and (b)  $w_1 = 1.6$  nm and (c) and (d)  $w_2 = 0.8$  nm, depending on whether the force field geometry optimization (MMFF, Spartan '18) was performed with or without the twelve  $\text{OC}_6\text{H}_{13}$  side chains (which may point to the intraannular lumen or the supernatant liquid phase).

The overview STM image of **1** (Figure S5a) shows two-dimensional (2D) crystalline domains in the size range of  $20 \times 20 \text{ nm}^2$ , however with some disorder regarding the lattice positions. Moreover, the bright oval-ish features in Figure S5a have rather inhomogeneous shapes. At first sight, we interpret these as dense and wide conformers, in which different numbers of alkoxy side chains fill the intraannular lumen (cf. Figure S4) and likewise the surface regions between the molecules.

The detail STM image shown in Figure 1a (Main Text) and Figure S5b is not resolved down to the alkoxy-chain level. Therefore, we refrain from an in-depth discussion of the sidechain interdigitation schemes, while an idealized model is shown in Figure 1c (Main Text). Nevertheless, the rigid rod segments of the backbones are clearly resolved and appear as bright features. The rod–rod distances of the 18 individual molecules seen in Figure S5b are listed in Table S1. Among these, only 3 molecules (cf. arrows 14, 15, and 17 in Figure S5b) have a width in the interval of 1.5 – 1.7 nm that matches the width  $w_1$  (of 1.6 nm) of the structure discussed in Figure S4a, where all alkoxy side chains pack densely in the intraannular lumen. Furthermore, only 1 molecule with a smaller width (of 1.4 nm) was observed. A width of 0.8 nm, corresponding to the conformer shown in Figure S4c and d, was not observed in the STM experiment. Unexpectedly, 15 molecules are even wider than the “wide” conformer predicted in Figure S4a: 8 molecules have widths in the interval of 1.8 – 2.0 nm (cf. arrows 2, 5, 6, 7, 9, 12, 15, and 16 in Figure S5b), and 6 molecules have widths in the interval of 2.0 – 2.2 nm (cf. arrows 1, 3, 4, 8, 10, and 11 in Figure S5b). Consequently, the alkoxy side chains in the intraannular regions pack even more loosely than predicted in the initial model in Figure S4a, and the nominally linear rigid rod units are even more bent.

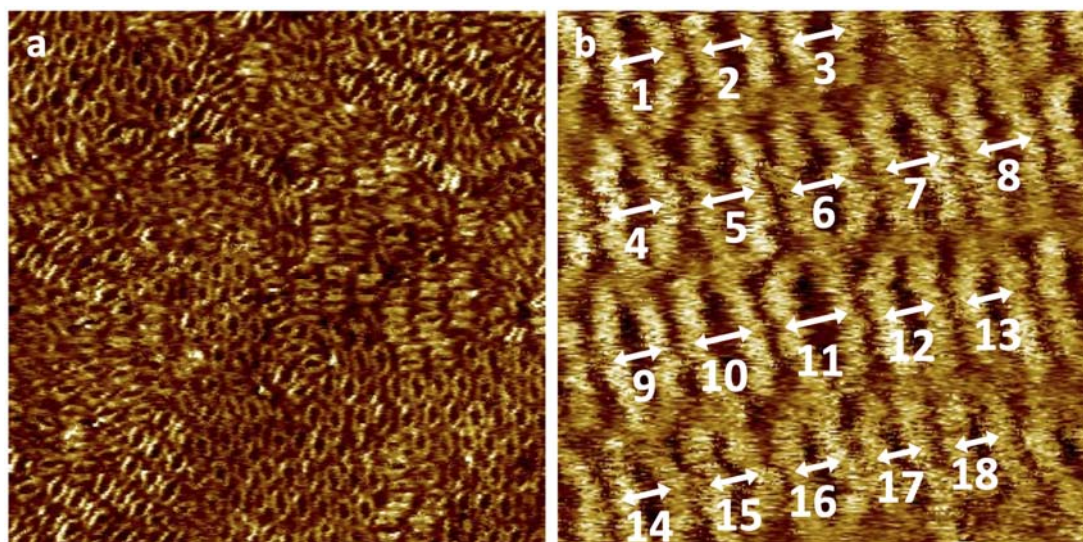


**Figure S5:** (a) Overview STM image of **1** at the solid/liquid interface of highly oriented pyrolytic graphite and a solution of **1** in 1,2,4-trichlorobenzene; (b) copy of the scanning tunneling microscopy image of **1** shown in Figure 1a (Main Text) with assignments. Image parameters of (a):  $100 \times 100 \text{ nm}^2$  (internal scanner calibration),  $V_s = -1.2 \text{ V}$ ,  $I_t = 26 \text{ pA}$ ; of (b):  $18 \times 18 \text{ nm}^2$ ,  $V_s = -0.8 \text{ V}$ ,  $I_t = 55 \text{ pA}$ ; both images:  $c = 5 \times 10^{-6} \text{ M}$ , sample thermally annealed for 20 s to  $80 \text{ }^\circ\text{C}$  prior to imaging. The arrows in (b) indicate the widths of molecules 1 – 18 discussed in Table S1.

Structure no.	Width/nm
1	2.1
2	2.0
3	2.1
4	2.2
5	1.8
6	2.0
7	1.8
8	2.1
9	1.8
10	2.1
11	2.2
12	2.0
13	1.8
14	1.7
15	1.6
16	1.8
17	1.6
18	1.4

**Table S1:** Widths of the rigid rod units of molecules 1-18 in Figure S5b.

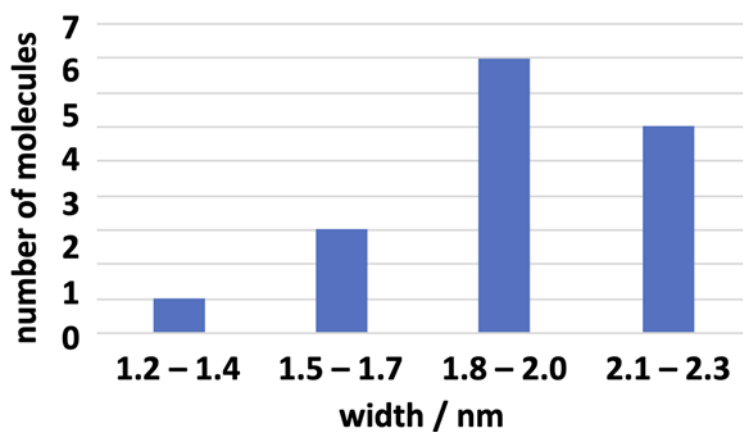


**Figure S6:** Numbers of molecules in Figure S5b that have widths in the given intervals.

The overview STM image of **8** (Figure S7a) is dominated by one- (1D) and 2D crystalline domains (with average sizes in the range of  $20 \times 20 \text{ nm}^2$ ). These are assembled of parallel aligned two-fold jagged linear species, attributed to the *trans/trans*-conformer of **8** (cf. space-filling model in Figure S7b and c) with a length,  $d_{\text{H-H}}$ , of 10.7 nm. Moreover, two other types of structures observed by STM are attributed to *cis/cis*-**8** at the domain boundaries, *i.e.* a U-shaped conformer of *cis/cis*-**1** (cf. arrow 1 in Figure S7a and space-filing model in Figures S7d and e) and a Z-shaped conformer of *cis/cis*-**1** (cf. arrows 2 to 7 and space-filing model in Figures S7f and g). (The space-filling models were obtained by force-field geometry optimization (MMFF, Spartan '18) from different starting geometries.)

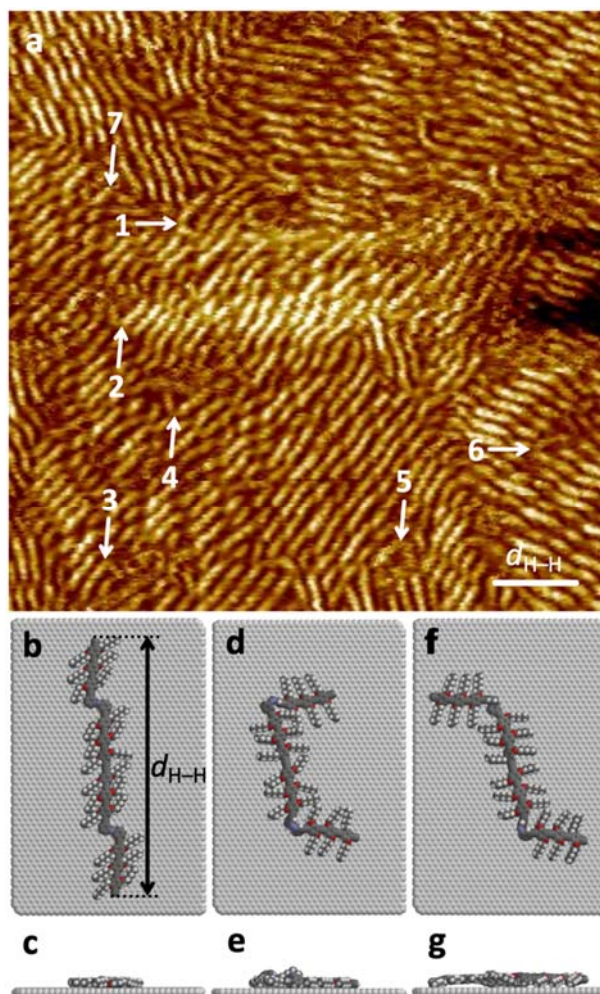


**Figure S7:** (a) Scanning tunneling microscopy image of **8** at the solid/liquid interface of highly oriented pyrolytic graphite and a solution of **8** in 1,2,4-trichlorobenzene; (b) – (e) space-filling models of single molecules of (b) and (c) *trans/trans*-**8** (with a length,  $d_{\text{H-H}}$ , of 10.7 nm), (d) and (e) a U-shaped conformer of *cis/cis*-**8**, marked by arrows 1 to 6 in (a); (f) and (g) a Z-shaped conformer of *cis/cis*-**8**, marked by arrow 7 in (a). Image parameters of (a):  $80 \times 80 \text{ nm}^2$  (internal scanner calibration),  $V_S = -1.1 \text{ V}$ ,  $I_t = 117 \text{ pA}$ ,  $c = 1 \times 10^{-5} \text{ M}$ , sample thermally annealed for 20 s to  $80 \text{ }^\circ\text{C}$  prior to imaging.

A schematic representation of **8** with respect to the degrees of freedom is shown in Figure S8. Both azobenzene units of **8** can (nominally) adopt *trans* or *cis* configuration (independently). Moreover, adsorption to the HOPG surface reduces the rotational degrees of freedom, and *anti* as well as *syn* conformations can be distinguished regarding the conformations of the rigid rod units relative to each of the azobenzene units. Moreover, the *anti* and *syn* conformations of both azobenzene units relative to the central rod can be distinguished.

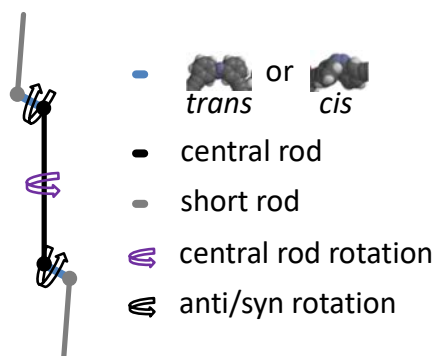


**Figure S8:** Schematic representation of the different units of **8** that can undergo *trans-cis*-isomerization and adopt *anti* or *syn* conformations after adsorption to the HOPG surface.

## 6. UV/vis spectra of **1**, **6b**, and **8**

Under the exclusion of light, a solution of  $6 \times 10^{-6}$  M of **1** in toluene was prepared and allowed to stand for 2 h in the dark before the UV/vis spectrum shown in Figure S9a, black solid line, was acquired. Irradiation of this solution for 10 s with a light emitting diode (InGaN-based LED, model APG2C1-410, continuous wave output power 125 mW, Roithner Lasertechnik, Vienna, Austria) with a peak wavelength of 410 nm and a FWHM of 20 nm did not lead to a spectral change (Figure S9a, red solid line), and neither changes were observed after extending the irradiation for 20 s (green dotted line), 200 s (blue dashed line) or with other LEDs at 254 nm, 310 nm, 515 nm, and 650 nm for 3 min, 450 nm for 6 min, and 532 nm for 10 min (not shown here).

When (under the same conditions, *i.e.* darkness) a solution of  $6 \times 10^{-6}$  M of **8** in toluene was prepared and allowed to stand for 2 h in the dark, the spectrum shown in Figure S9b (black solid line) was recorded. The irradiation with the same LED at 410 nm for 10 s led to a minor change in the blue region of the spectrum shown in Figure S9b (red solid line). (Note, that in another experiment (not shown here) we observed identical UV/vis spectra after irradiating a  $\approx 6 \times 10^{-6}$  M solution of **8** for 5 s and extending the irradiation to 10 s with the same LED at 410 nm, therefore saturation is reached.) Allowing the solution of **8** (after 10 s irradiation at 410 nm) to stand for 5 h at rt led to a slight shift in intensity (Figure S9b, blue dotted line), however not to a complete recovery of the initial spectrum within the given timeframe. However, in the  $^1\text{H}$  NMR spectrum (Figure S2), it is clearly visible that at elevated temperatures (100 °C) exclusively the *trans*-isomer is observed. (Nevertheless, heating of the solution in the UV/vis cuvette was not feasible due to concentration changes and minimal spectral changes.)

Moreover, (in darkness) a solution of  $6 \times 10^{-6}$  M of **6b** in toluene was prepared and allowed to stand for 2 h in the dark, before the spectrum shown in Figure S9c (black solid line) was recorded. Irradiation with 410 nm for 5 s led to a shift in intensity (red solid line) and no further intensity change was observed after extending the irradiation to 10 s (green dotted line). Allowing the solution to stand for 5 h led to a shift in intensity (Figure S9c, blue solid line), however not to a complete recovery of the initial spectrum.

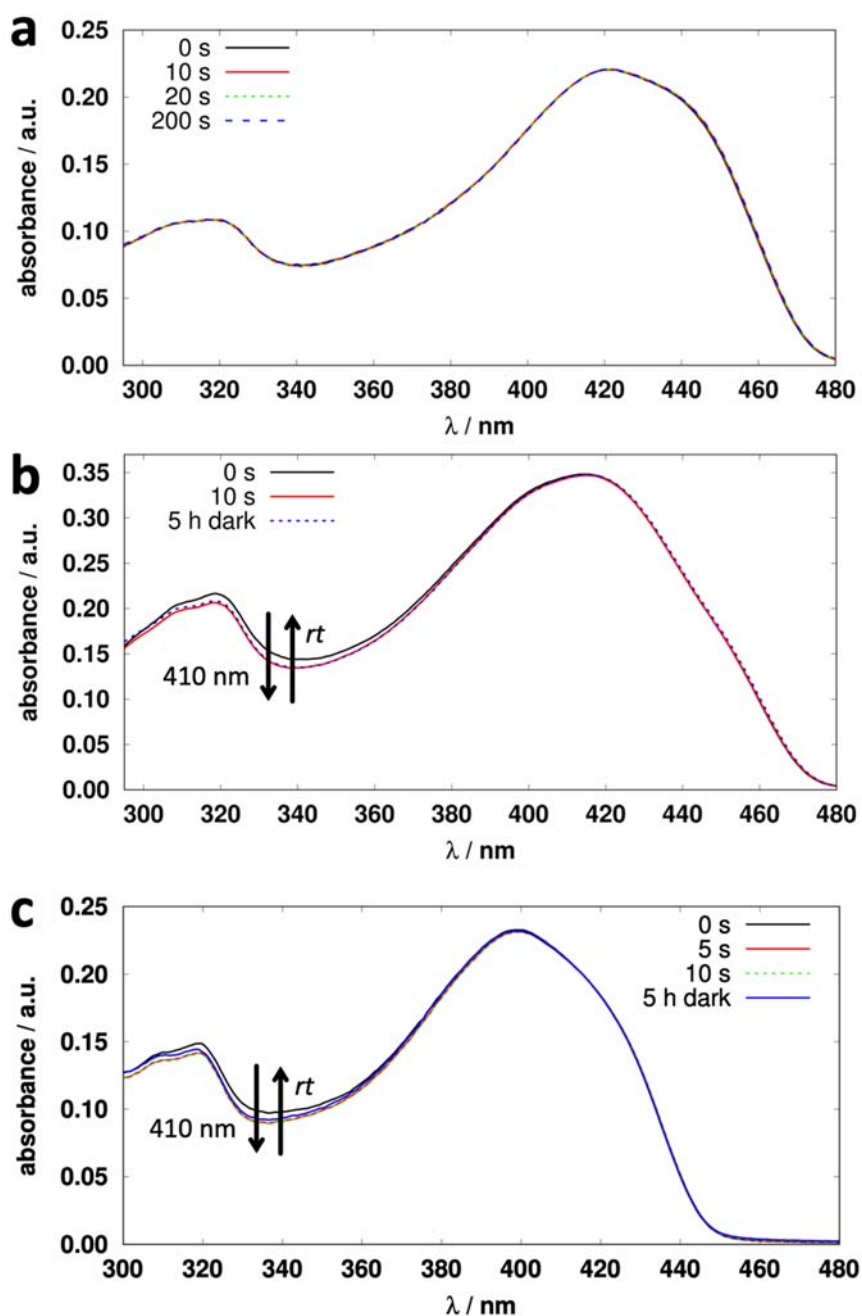


**Figure S9:** UV/vis spectra of (a) **1** (black line: after preparing a  $6 \times 10^{-6}$  M solution of **1** in toluene and allowing this solution to stand for 2 h in the dark; red solid/green dotted/blue dashed lines: after 10 s/20 s/200 s irradiation at 410 nm); (b) **8** (black solid line: after preparing a  $6 \times 10^{-6}$  M of **8** in toluene and allowing this solution to stand for 2 h in the dark; red solid line: after 10 s irradiation at 410 nm; blue dotted line: after 5 hours at rt in the dark); (c) **6b** (black solid line: after preparing a  $6 \times 10^{-6}$  M of **6b** in toluene and allowing this solution to stand for 2 h in the dark; red solid line: after 5 s irradiation at 410 nm; green dotted line: after extending irradiation time to 10 s (at 410 nm); blue solid line: after allowing the solution to stand in the dark at rt for 5 h).

Under exclusion of light, a solution of  $6 \times 10^{-6}$  M of **8** in toluene was prepared and allowed to stand for 2 h in the dark before the UV/vis spectrum shown in Figure S10a, black solid line, was acquired. Irradiation of this solution for 5 s with a light emitting diode (CHTPON, China; 3-4 mW continuous output power) with a peak wavelength of 310 nm and a FWHM of 10 – 12 nm led to a minor change in the spectrum (red dashed line) that gradually increased when the irradiation was extended to 10 s (blue dotted line) and 60 s (green dotted line). However, no further change was observed when the irradiation was extended to 90 s (pink dashed line).

When (under the same conditions, *i.e.* darkness) a  $6 \times 10^{-6}$  M of **6b** in toluene was prepared and allowed to stand for 2 h in the dark, the UV/vis spectrum shown in Figure S10b (black solid line) was recorded. The irradiation with the same LED at 310 nm for 5 s led to a minor change in the spectrum (red dashed line), that gradually increased when the irradiation was extended to 10 s (blue dotted line) and 60 s (green dotted line). However, no further change was observed when the irradiation was extended to 90 s (pink dashed line).

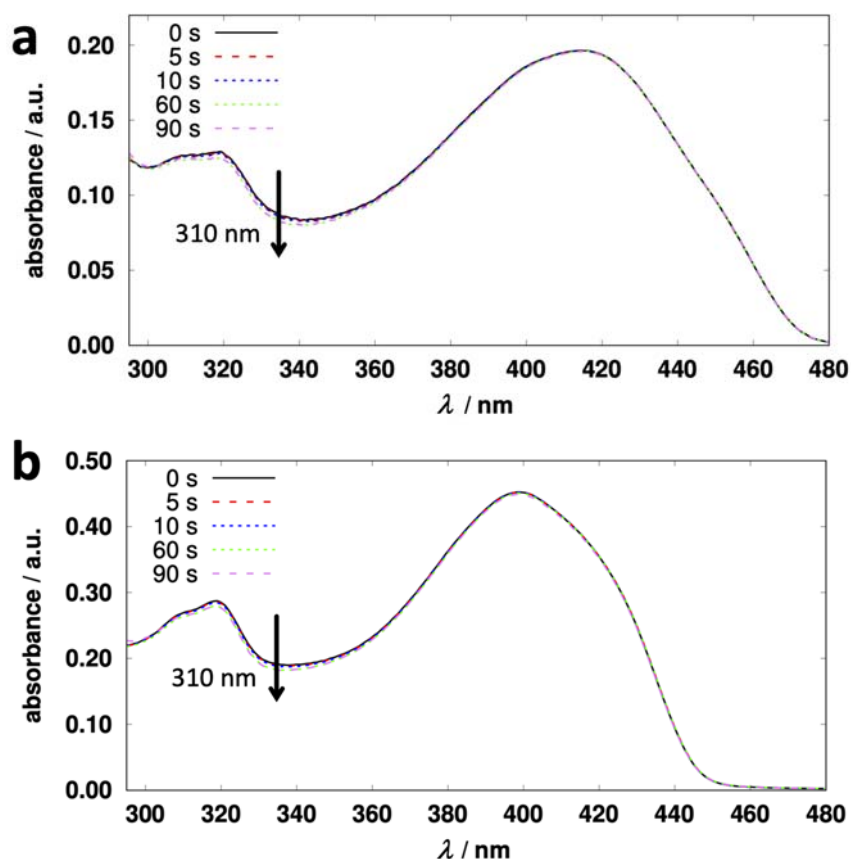


**Figure S10:** UV/vis spectra of (a) **8** (black solid line: after preparing a  $6 \times 10^{-6}$  M solution of **1** in toluene and allowing this solution to stand for 2 h in the dark; red dashed/blue dotted/green dotted/pink dashed lines: after 5 s/10 s/60 s/90 s irradiation at 310 nm); (b) **6b** (black solid line: after preparing a  $6 \times 10^{-6}$  M solution of **6b** in toluene and allowing this solution to stand for 2 h in the dark; red dashed/blue dotted/green dotted/pink dashed lines: after 5 s/10 s/90 s irradiation at 310 nm).

Figure S11 shows UV/vis spectra of 2,2'-diiodoazobenzene (**3**) and the rigid rod reference compound **19** having the same length as the (long) rigid rod units in **1** and **8**. (Note that the synthesis of **19** is described in Ref. [S4].) **19** has an absorption maximum at 400 nm (whereas the absorption maximum of **1** is at 421 nm). The extinction coefficient,  $\epsilon$ , of **19** at 400 nm is  $51.1 \times 10^3 \text{ M}^{-1} \text{ cm}^{-1}$ . However, diiodoazobenzene in the wavelength range of 390–420 nm has an extinction coefficient close to zero. Accordingly, we expect that when **1**, **6a**, or **8** is irradiated at 410 nm (cf. Figure S9), the absorption is dominated by the rigid rod unit. Taking into account the low UV content in daylight (or laboratory light), the absorption and therefore *cis-trans*-switching (cf. Figures S12-S15) after exposure to daylight is attributed to the absorption of the oligo(*p*-phenylene-ethynylene-butadiynylene)s units.

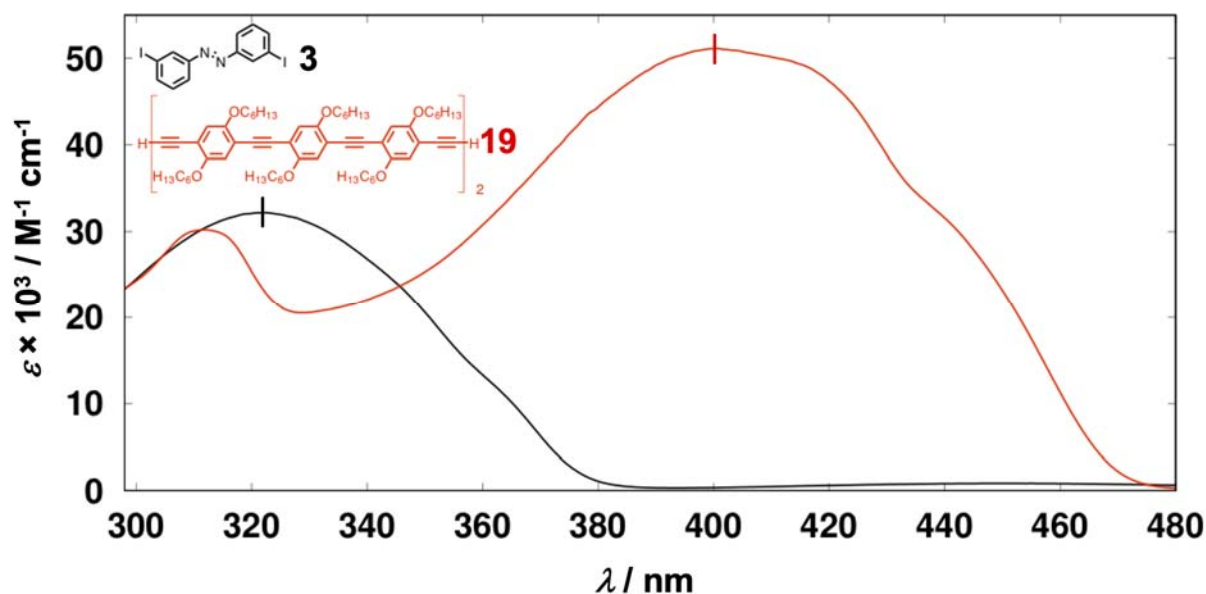


**Figure S11:** UV/vis spectra of **3** (black line) and **19** (red line). Extinction coefficients at the maxima are for **3** ( $\lambda = 322 \text{ nm}$ ):  $\epsilon = 32.2 \times 10^3 \text{ M}^{-1} \text{ cm}^{-1}$ , for **19** ( $\lambda = 400.5 \text{ nm}$ ):  $\epsilon = 51.1 \times 10^3 \text{ M}^{-1} \text{ cm}^{-1}$ .

## 7. Thin layer chromatography of **6b** and **8**

The macrocycle precursor **8** (containing two azobenzene units) and a half-ring structure **6b** (containing one azobenzene unit) were investigated by two-dimensional thin-layer chromatography (2D-TLC) using Cy:DCM 1:2 as mobile phase.

**8** was dissolved in DCM, and the solution was spotted on a TLC plate in daylight. Under exclusion of light, a first run (from right to left direction in Figure S12a) and a subsequent second run (from bottom to top in Figure S12a, without intermediate illumination) ultimately yielded two discrete spots ( $R_f = 0.37$  and  $0.51$ ) marked in orange in Figure S12a, left panel). From this experiment, we conclude that **8** – in daylight – adopts two switching states that do not interconvert in darkness (*e.g.* during the TLC run).

Subsequently, **8** was dissolved in DCM and spotted on the TLC plate in daylight. A first development in darkness (from right to left, Figure S12b) yielded two spots ( $R_f = 0.21$  and  $0.33$ , marked in yellow), attributed to the presence of two states of **8** in the solution and no further switching during the first TLC run. After the first run, the TLC plate was exposed to daylight (for 2 min), and the TLC plate was again developed in darkness (from bottom to top). During this procedure, each of the two spots split up into a series of another two spots ( $R_f = 0.12$  and  $0.29$ , marked in orange). We conclude that the two states (of the molecules on the TLC plate) interconvert into each other. At present, it remains speculative why only two states are distinguishable despite the system having two azobenzene switches, implying that nominally three states should exist.

(Note that  $R_f$  values for the respective second runs of the 2D-TLC experiments may differ from the values for the respective initial runs due to the ratio of the mobile phase throughout both runs not being constant.)

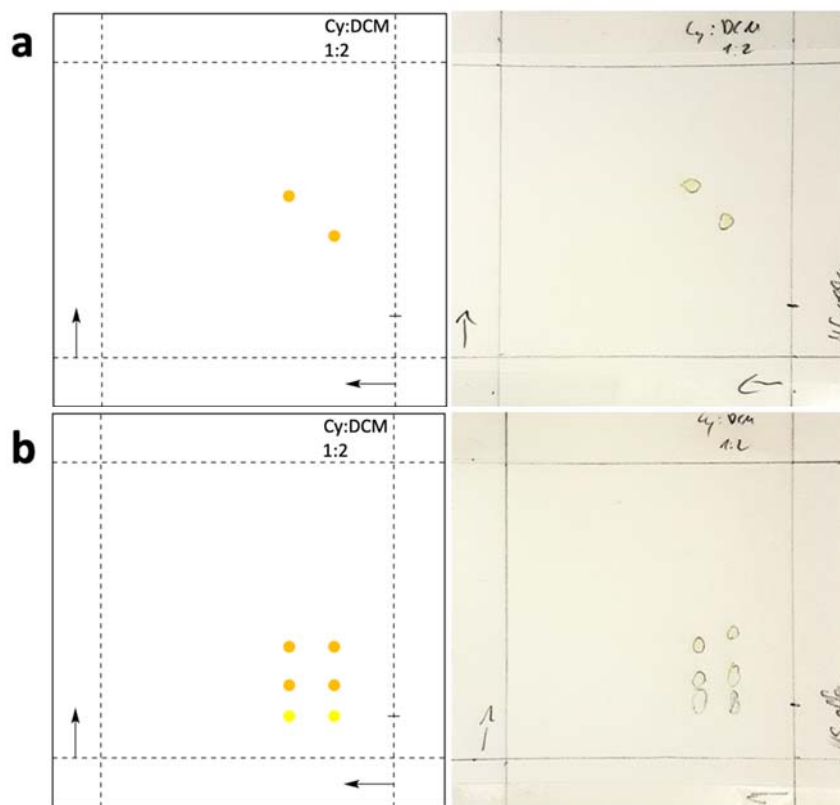


**Figure S12:** Two-dimensional thin layer chromatography of **8** (Cy:DCM 1:2) performed under different light conditions; 1<sup>st</sup> run: from right to left; 2<sup>nd</sup> run: from bottom to top. (a) **8** dissolved and spotted on the TLC plate in daylight, and the TLC developed in darkness; (b) **8** dissolved and spotted on the TLC plate in daylight, developing the TLC (from right to left direction) in darkness, illuminating the TLC (for 2 min in daylight), and developing the TLC (from bottom to top) in darkness.

In addition, three solutions of **8** were subjected to different illumination conditions prior to performing one-dimensional (1D) TLC using Cy:DCM = 1:2 as a mobile phase in darkness. A first sample was dissolved (in DCM) in daylight, spotted on the TLC plate ("l" in Figure S13) and separated (after the TLC run) into two discrete spots ( $R_f = 0.21$  and  $0.33$ ), attributed to two switching states. A second sample was dissolved (in DCM) in darkness and illuminated for 2 min with a 410 nm LED before being spotted on the TLC plate ("410" in Figure S13). This led to two spots (with the same  $R_f$  values as in the experiment before) after the TLC run. A third sample was dissolved and applied to the TLC plate in darkness ("d" in Figure S13) and yielded only one spot ( $R_f = 0.33$ ).

The results indicate that storing the compound in the dark for longer time leads to one isomer, most probably the *trans/trans*-isomer. Illumination by either daylight or a 410 nm LED leads to population of the same state and another state with higher dipole moment. Unexpectedly, a third state is not observed.

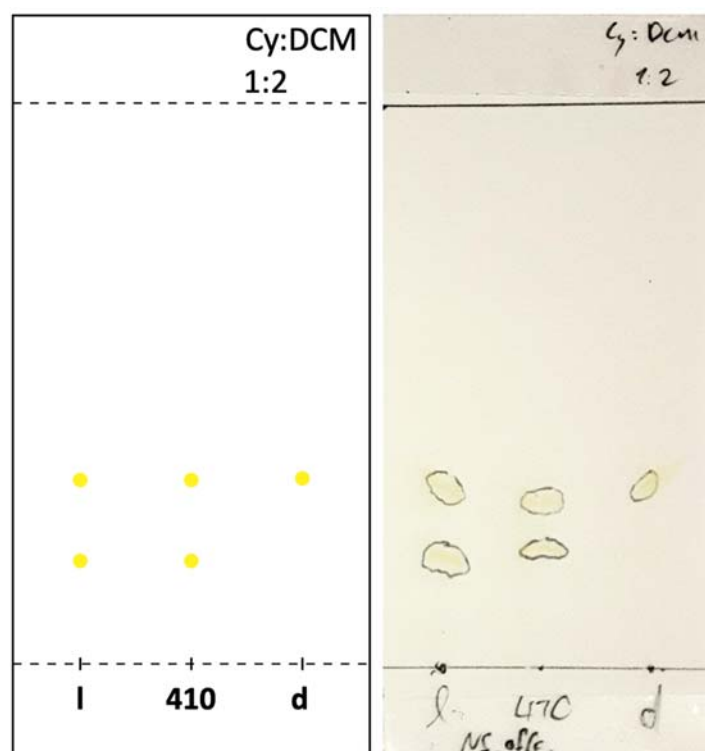


**Figure S13:** Two-dimensional thin layer chromatography of **8** in Cy:DCM 1:2 after treatment of **8** in different illumination conditions and performing a subsequent TLC run in darkness. l: **8** was dissolved and applied to the TLC plate in daylight; 410: **8** was dissolved in darkness, the solution was illuminated with a 410 nm LED for 2 min, and the solution was applied to the TLC plate in darkness; d: **8** was dissolved and applied to the TLC plate in darkness.

**6b** was dissolved in DCM under exclusion of light and the solution was spotted on the TLC plate. Still in darkness, a first run in Cy:DCM 1:2 (from right to left direction in Figure S14a) and a subsequent second run (from bottom to top in Figure S14a, still in darkness) yielded one discrete spot (marked in orange in Figure S14a, left panel). (Note that the yellow spot in Figure S14a, left panel, marks the expected position of **6b** after the first TLC run. Note also that we refrain from quantifying the exact  $R_f$ -values here, as the exact positioning of the compound is not possible in the dark.) From this experiment, we conclude that **6b** – in complete darkness – adopts one switching state that does not change during the procedure.

Then, **6b** was dissolved and applied to the TLC plate in DCM in daylight. A first and second development in darkness in Cy:DCM 1:2 (in orthogonal directions) yielded two spots ( $R_f = 0.25$  and  $0.47$ , Figure S14b), attributed to the presence of two states of **6b** in the original solution and no further switching during the two TLC runs.

When **6b** was dissolved and applied to the TLC plate in DCM in daylight, a first TLC run in daylight (from right to left) yielded the smeared spot ( $R_f = 0.47$ ) marked in yellow (Figure S14c, left panel), and a second run (from bottom to top) yielded the smeared spot marked in orange. We attribute this behavior to back and forth switching both in solution and on the TLC plate.

**6b** was then dissolved and applied to the TLC plate in DCM in daylight. A first TLC run in darkness (in Cy:DCM 1:2, from right to left) yielded two discrete spots ( $R_f = 0.22$  and  $0.46$ ) marked in yellow in Figure S14d, left panel. When the TLC plate was illuminated by daylight, and a second run was performed in darkness (from bottom to top), each of the two spots split up into another pair of spots ( $R_f = 0.15$  and  $0.38$ ). We attribute this to the presence of two distinguishable states in the original solution of **6b**, which interchange during illumination.

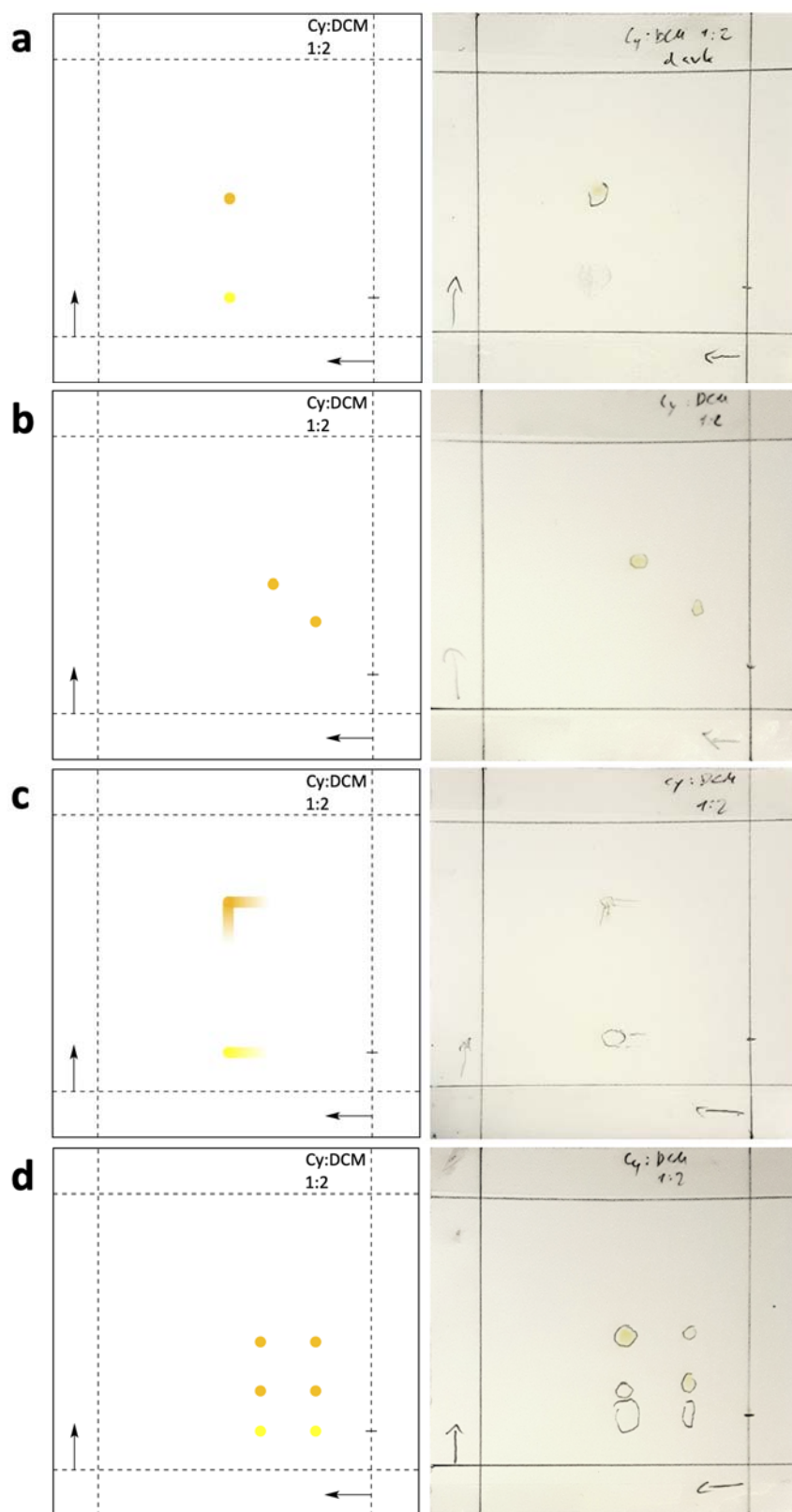


**Figure S14:** Two-dimensional thin layer chromatography of **6b** (Cy:DCM 1:2) performed under different light conditions; 1<sup>st</sup> run: from right to left; 2<sup>nd</sup> run: from bottom to top. (a) **6b** dissolved and developed in darkness; (b) **6b** dissolved in daylight and developed in darkness; (c) **6b** dissolved and developed in daylight; (d) **6b** dissolved in daylight, developed in darkness, illuminated by daylight, rotated by 90° and developed in darkness.

Three solutions of **6b** in DCM were subject to different illumination conditions, before a 1D TLC using Cy:DCM = 1:2 as the mobile phase was developed in darkness. A first sample of **6b** was dissolved and applied to a TLC plate in darkness (“l” in Figure S15) and led (after the TLC run) to two discrete spots ( $R_f = 0.24$  and  $0.46$ ), attributed to two switching states. A second sample was dissolved in darkness and illuminated for 60 s with a 410 nm LED for 60 s before being applied to the TLC plate (“410” in Figure S15), and led to two identical spots after the TLC run. A third sample was dissolved and applied to the TLC plate in darkness (“d” in Figure S15) and yielded only one spot ( $R_f = 0.46$ ).

The results indicate that the absence of illumination leads to population of only one state, while illumination by either daylight or a 410 nm LED leads to population of the same state and a second state with higher dipole moment.

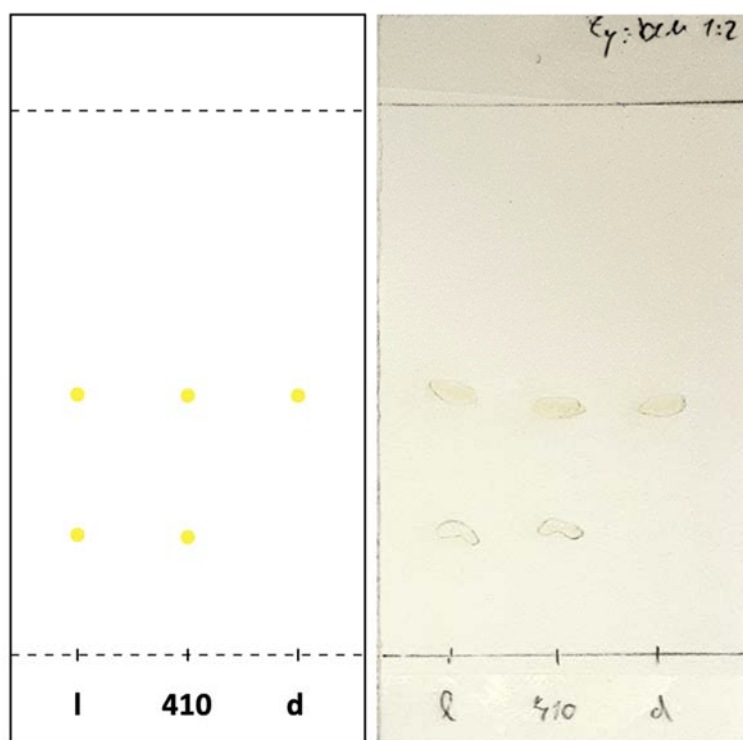


**Figure S15:** Two-dimensional thin layer chromatography of **6b** in Cy:DCM 1:2 after treatment of **6b** (in DCM) in different illumination conditions and performing a subsequent TLC run in darkness. l: **6b** was dissolved and applied to the TLC plate in daylight; 410: **6b** was dissolved in darkness, the solution was illuminated with a 410 nm LED for 60 s, and the solution was applied to the TLC plate in darkness; d: **6b** was dissolved and applied to the TLC plate in darkness.

## 8. Optical spectroscopy

Figures S16a and b show histograms of the PL lifetimes of the azobenzene clamped bichromophore, **1**, and the rigid-clamp bichromophore, **2**. Figures 16c and d show the arrival time differences between two consecutively detected photons in intervals of the laser-pulse repetition period (12.5 ns).

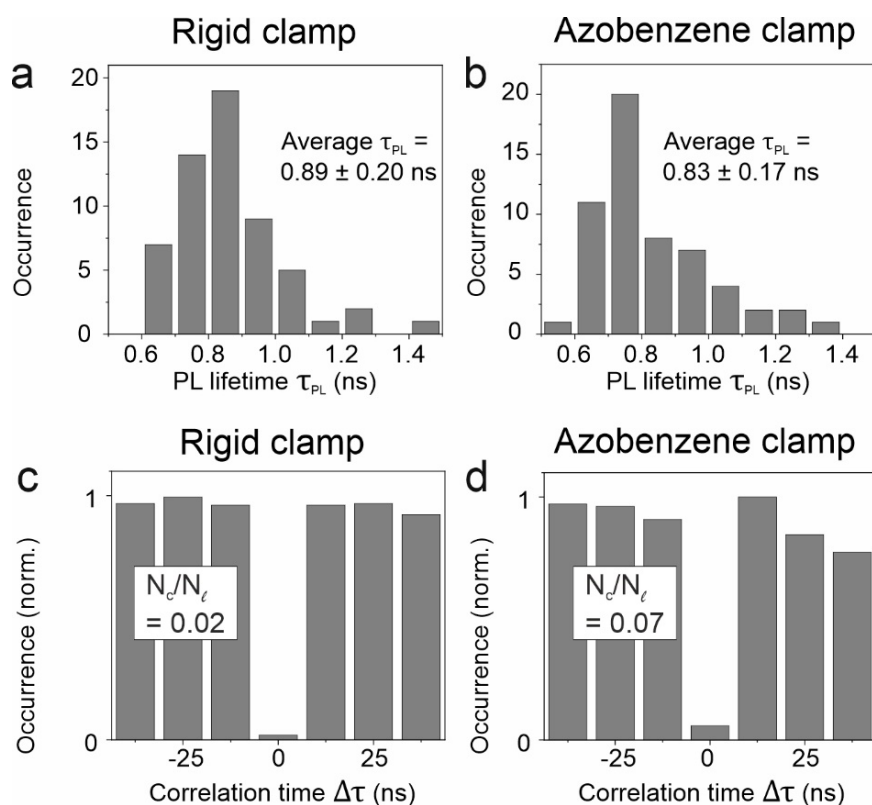


**Figure S16:** Additional single-molecule measurements: (a) and (b) show histograms of the measured PL lifetimes of the rigid-clamp bichromophore structure **2** and the azobenzene clamped bichromophore **1**, respectively. The average values are stated in the plots together with the standard deviations. (c) and (d) show histograms of the arrival time difference between two consecutively detected photons in intervals of the laser-pulse repetition period (12.5 ns). Both the rigid-clamp structures **2** (c) and azobenzene clamped bichromophore **1** (d) show nearly perfect single photon emission, *i.e.* an absence of a photon correlation signal at zero delay time, quantified by the ratio between the central and lateral values  $N_c$  and  $N_\ell$  of the histogram. The average values are stated in the plots. The histograms are averaged over 21 (c) and 30 (d) single molecules.

## 9. References

[S1] Höger, S. *Liebigs Ann./Recueil* **1997**, 273.

[S2] a) Höger, S.; Bonrad K. *J. Org. Chem.* **2000**, 65, 2243; b) Gaefke, G.; Höger, S. *Synthesis* **2008**, 14, 2155.

[S3] Lee, S.; Hua, Y.; Flood, A. H. *J. Org. Chem.* **2014**, 79, 8383.

[S4] Jester, S.-S.; Schmitz, D.; Eberhagen, F.; Höger, S. *Chem. Commun.* **2011**, 47, 8838.

[S5] Ohlendorf, G.; Mahler, C. W.; Jester, S.-S.; Schnakenburg, G.; Grimme, S.; Höger, S. *Angew. Chem. Int. Ed.* **2013**, 52, 12086.

[S6] Meißner, S. A.; Eder, T.; Keller, T. J.; Hofmeister, D. A.; Spicher, S.; Jester, S.-S.; Vogelsang, J.; Grimme, S.; Lupton, J. M.; Höger, S. *Nat. Commun.* **2021**, 12, 6614.